Giant, 6, 2021, 100054

Review

Covalent organic frameworks: Design principles, synthetic strategies, and diverse applications

Hesham R. Abuzeid, Ahmed F.M. EL-Mahdy, Shiao-Wei Kuo*

Department of Materials and Optoelectronic Science, Center of Crystal Research, National Sun Yat-Sen University, Kaohsiung 80424, Taiwan

Keywords: Covalent organic frameworks (COFs), Porous materials, Energy storage, CO_2 uptake

Covalent organic frameworks (COFs) are the emerging type of organic crystalline porous materials, prepared through reticular chemistry with building blocks featuring light elements (such as C, H, O, N, or B atoms), and connected through the covalent bond and extended into two or three dimensions. In the past few years, COFs have attracted attention for their interesting properties, including high-order porosity, structural versatility, facile surface modification, and high thermal and chemical stabilities. Accordingly, COFs are potential platforms for diverse practical implementations, including gas separation and storage, heterogeneous catalysis, chemical sensing, luminescence, electronic devices, drug delivery, and energy storage and conversion. This Review provides the overview of the design strategies and synthetic methodologies that have been used widely for the preparation of COFs, and also summarizes selected examples of their applications.

1 Introduction

Nature inspires scientists to create new materials with complex structures that can perform advanced functions. Mimicking natural structures, scientists have explored an array of chemical architectures by connecting diverse building units through various strategies [1-3]. These efforts have resulted in many classes of porous materials, including mesoporous zeolites [4-5], silicas [6-8], phenolic resins and carbons [9-13], organosilicas [14-15], conjugated microporous polymers [16-19], and metal organic frameworks (MOFs) [20-21]. The formation of these structures depends mainly on the kinetically controlled irreversible coupling reaction, which can induce structural disorder and produce oligomer that decrease the efficiency of the processes [22]. As a result, there remains a need for new permanent porous materials having long-range-ordered structures and high crystallinity.

The covalent organic framework (COFs) were introduced by Yaghi et al. as the new type of crystalline porous organic polymers synthesized through reversible condensations of building blocks comprising light elements and connected by robust covalent bonds [23]. The self-healing ability of COFs and their thermodynamically controlled covalent bonding result in long-range-ordered crystalline structures. Moreover, COFs can exhibit excellent chemical stability in organic solvents and withstand harsh conditions (*e.g.*, acidic and basic conditions) to maintain their ordered structures and crystallinity. Such high stability results from the purely covalently bonded and metal-free structures of COFs (in comparison, MOFs are based on coordinative bonds) [24-25]. Furthermore, hydrogen bonds and π-stacking interactions in COFs can further strengthen their porous skeletons and protect them from solvation and hydrolysis [22,26]. Moreover, COFs can feature higher porosities and larger

* Corresponding author.
E-mail address: kuosw@faculty.nsysu.edu.tw (S.-W. Kuo).

Received 18 November 2020; Received in revised form 18 February 2021; Accepted 19 February 2021

https://doi.org/10.1016/j.giant.2021.100054

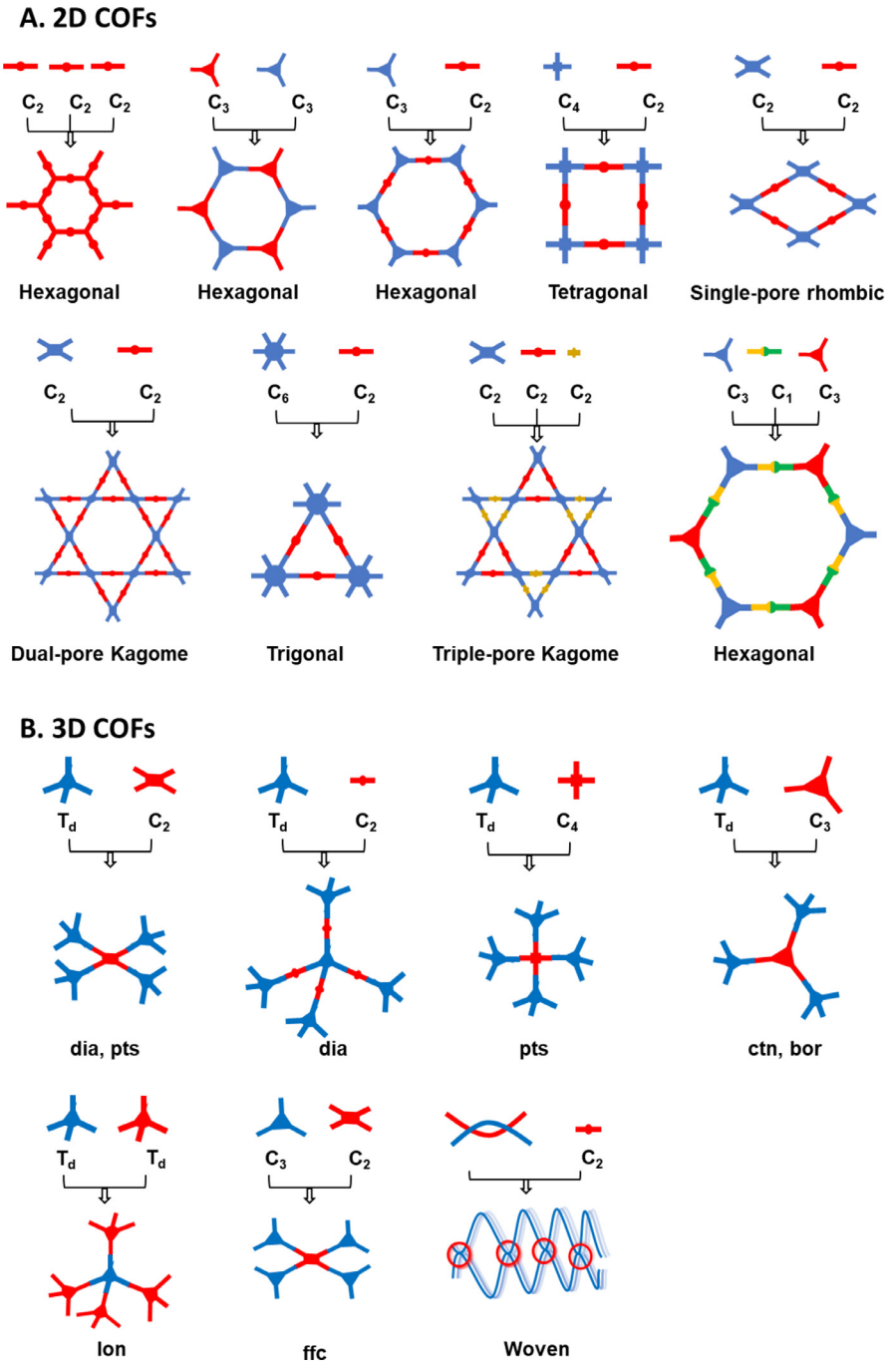

Fig. 1

Topology diagrams representing a general basis for COF design and construction of (A) 2D COFs and (B) 3D COFs.

pores than corresponding inorganic zeolites and other porous silicas, making them favorable for use in, for example, catalysis, where larger pores accelerate the diffusion of reactant and the desorption of product, thereby enhancing product yield and selectivity [27].

Several approaches have been developed to construct COFs with diverse topologies from various building units (**Fig. 1**). Theoretically, the topology of a COF is pre-determined by the dimensions and geometry of its building unit. The ability to predict the skeleton structures of COFs is unique, when compared with other porous materials; it enables the construction of complex geometries with highly ordered structures, rather than primary-ordered structures [28–30]. The topology diagram in **Fig. 1** provides a systematic method for generating polygons through integration of building units to form extended lattices in two-dimensional (2D) or three-dimensional (3D) COFs, yielding crystalline networks with alternately placed linkers and knots [31,32]. In this Review, we provide the overview of the basic

principles behind the design of COFs and the strategies that have been used for their construction. Furthermore, we discuss and compare the synthetic methodologies that have been developed so far. In addition, we provided an overview of the outstanding ability of COFs as platform for diverse applications. Specifically, we selected few examples of the applications of COFs to tackle energy-related challenges; including catalytic process to reduce the energy waste, reduction of carbon emission and energy storage and conversion. We also provided a focused discussion of design strategies toward COFs that can be used to improve the charge carrier transport and photoconductive properties of photovoltaic cells. This review seeks to encourage scientists from different backgrounds to explore COFs materials as platform for various applications.

2 Design principles and bond formation

The reversible nature of some of the covalent bonds in organic assemblies facilitates the formation of COFs with crystalline structures, because they allow error corrections and the rearrangements of lattice networks through the breaking and reforming of their bonds—a characteristic that is not available in amorphous polymers. Yaghi et al. pioneered the study of COFs through the co-condensation of boronic acids and catechol to form the five-membered boronic esters as connectors between the building units, as well as through the self-condensation of boronic esters to form boroxines [23]. Nevertheless, because boronic esters and boroxines are both sensitive to hydrolysis, there was an inherent preference to develop structures from more stable coupling units. Accordingly, many alternative reactions and synthetic routes have been developed. **Fig. 2** illustrates the most commonly used organic reactions. Among them, the production of stable COFs has been achieved by introducing imino bonds, through the condensation of aldehydes and amines, and by introducing hydrazones, azines, and imides. Moreover, the chemical stability has been improved with the synthesis of β-ketoenamines from 1,3,5-triformylphloroglucinol (TFP-3OHCHO) and primary amines, through irreversible enol–keto tautomerization, creating robust networks that resist strong acids and bases [33].

The structures and pores of COFs are mainly predetermined through geometric matching of the building units used to form polygonal skeletons. The shapes of the polygons and the pore sizes depend on the geometries and dimensions of the knots and linkers [28]. For example, condensation of a building unit of C_3-symmetry with a linear linker of C_2-symmetry ($C_3 + C_2$) provides to the formation of an hexagonal COF [23,34]. Furthermore, hexagonal COFs could be synthesized through self-condensation of the C_2-symmetric unit [23,35,36]. Moreover, the use of two building units having a trigonal planar $C_3 + C_3$ geometry leads to a hexagonal COF [37–42]. The co-condensation of tetragonal building units with linear linkers ($C_4 + C_2$) can produce sheets featuring tetragonal pores. Those pores generate extended one-dimensional (1D) channels through stacked layers that extended in two directions. This unique structure enables the preparation of a variety of π-conjugated frameworks [43,44]. When the layers of a COF extend in two dimensions, the material is called a 2D COF (**Fig. 1A**); a 3D COF results from the building units forming a net in three dimensions (**Fig. 1B**). The $C_2 + C_2$ topology scheme leads to one of two possible structures: a rhombic-shaped skeleton [29,45] or a kagome structure [46–48]; the final polygonal structure is determined by the π-structure of the vertical construction.

Fig. 1 illustrates the construction principles of 2D and 3D COFs. The preparation of 2D COFs possessing dense π-units and micropores, necessary for the development of π-stacked organic polymers and porous materials, has been achieved using a $C_6 + C_2$ topology scheme, which allowed the construction of triangular lattices featuring highly dense π-units and smaller pores when compared with all of the other topology diagrams. As a rule of thumb, a trigonal structure is usually for producing microporous COFs, while tetragonal and hexagonal topologies are useful designing mesopores [49]. Interestingly, kagome-type COFs featuring triple pores have been constructed from one knot with two linkers of different lengths, in a $C_2 + C_2 + C_2$ topology diagram [50]. The condensation of asymmetric building blocks [44] or the introduction of hydrogen bonds in the COF skeleton [41] enhances the formation of COFs having dual-pore hexagonal structures. The introduction of asymmetric topology is based on multi-components concept in which two or three linkers is used to connect knots, this strategy increases the diversity of the resultants COFs and enhance the complexity of COFs structure [51,52]. For example, (1 + 2) three-components strategy generate COFs featured two different types of hexagonal structure, depending on the molar ration of the linkers. This method is achieved by introduction desymmetry units which possess arms with different lengths, this leads to formation of pores with different shape and size [53]. For example, two COFs (SIOC–COF-1 and SIOC–COF-2) was synthesized using condensation of two dialdehydes of different lengths and the same molarity to TPE knot (4,4′,4″,4‴-(ethene-1,1,2,2-tetrayl)tetraaniline (ETTA)) [54]. In comparison with 2D COFs which requires planar units, the construction of 3D COFs often requires at least one knot having orthogonal with C1, C2, C3, C4 or T_d symmetry to support the extended covalently linked 3D network and form skeletons and pores (**Fig. 1B**). 3D COFs have been designed to follow a variety of topologies, including dia, bor, rra, ctn, ffc, srs, and pts nets. The largest number of 3D COFs have been constructed using a $C_2 + T_d$ topology system, which has provided COFs with dia networks [55–59]. By changing these C_2-symmetric monomers functionalized with two reactive groups to other C_2-symmetric monomers having four reactive groups, 3D COFs with pts nets have been obtained. The 3D COFs with pts networks can also result from a $C_4 + T_d$ topology system [60–62]. Recently, the $C_3 + T_d$ topology system has been employed to fabricate 3D COFs with bor and ctn networks. For example, when the T_d-symmetric linkers tetra(4-dihydroxyborylphenyl)silane (TBPS) and tetra(4-dihydroxyborylphenyl)methane (TBPM) underwent self-assembly, 3D COFs having ctn nets were obtained, whereas the co-polycondensation of TBPM with C_3-symmetric linkers provided 3D COFs having a bor network [63–67]. The $C_3 + T_d$ topology system has also been applied to produce an srs net 3D COF [68]. The $C_3 + C_2$ topology diagram has been used to prepare a unique example of a 3D COF having an ffc net [69]. In 2016, a woven 3D-COF, named COF-

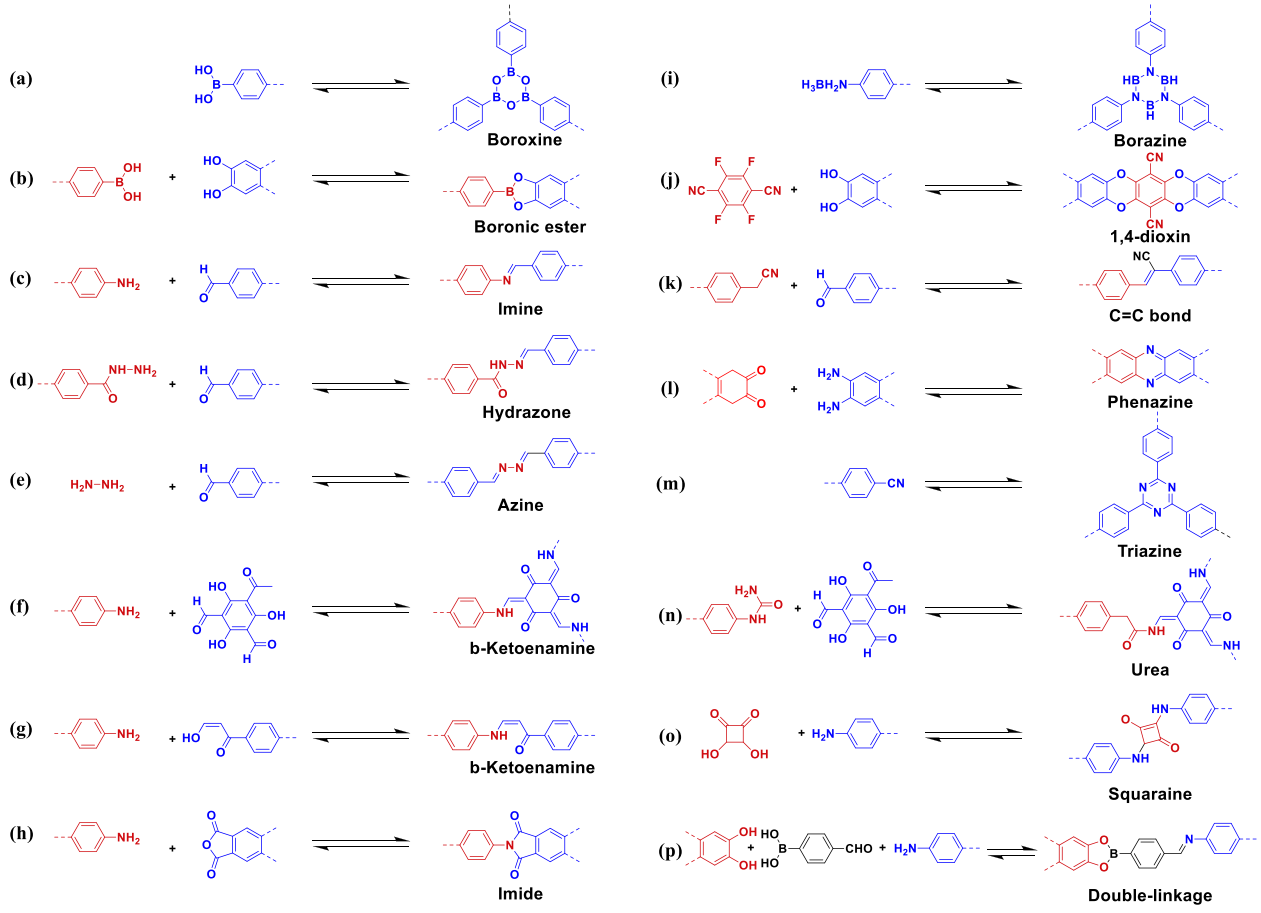

Fig. 2

Condensations of widely used types of linkages in COFs: (a) boroxine, (b) boronic ester, (c) imine, (d) hydrazone, (e) azine, (f, g) β-ketoenamine, (h) imide, (i) borazine, (j) 1,4-dioxin, (k) $C=C$ bond, (l) phenazine, (m) triazine, (n) urea, (o) squaraine, and (p) double-linkage.

505, has been constructed using helical organic threads by the simple imine polycondensation of benzidine (BZ) with copper(I)-bisphenanthroline tetrafluoroborate ($Cu(PDB)_2(BF_4)$) which possess four aldehydic groups [70]. The topology diagram in **Fig. 1** can be considered as the general basis for the construction and design of COFs. The high design ability of COFs is a feature that is difficult to achieve in other porous materials. Therefore, COFs are the attractive materials that have diverse structures and functions.

3 Linkage types of COFs

3.1 Boron-containing COFs

Since the pioneering studies into the synthesis of COFs by Yaghi and his group [23], diverse boron-containing COFs have been constructed using boronated esters or boronated anhydrides. The resulting COFs have been classified into two categories based on the condensation strategy. The first comprises COFs prepared though self-condensation of a single building block, yielding cyclic six-membered boroxine-linked COFs (**Fig. 2(a)**). For example, the self-condensation of 1,4-benzenediboronic acid yielded the 2D COF-1, featuring highly crystalline and expanded porous 2D graphitic layers, with high surface area of 711 $m^2\ g^{-1}$. Similarly, the 3D COF-103, synthesized through self-condensation of TBPS with a high surface area of 4210 $m^2\ g^{-1}$ (**Fig. 3(a)**) [17]. The other category of boron-containing COFs comprises those constructed through co-condensation of boronic acids and catechol derivatives, leading to five-membered ring boronate esters (**Fig. 2(b)**). By varying the boronic acid and diol building blocks, COFs have been obtained displaying diverse properties and functionalities. For example, Dichtel et al. synthesized HHTP-DPB COF through solvothermal co-condensation of 2,3,6,7,10,11-hexahydroxytriphenylene (HHTP) and 4,4-diphenylbutadiynebis(boronic acid) (DPB); this COF (**Fig. 3(b)**) featured a high surface area (930 $m^2\ g^{-1}$) and a large pores (4.7 nm) [71]. The high crystallinity of boronate ester COFs encourages the integration of electron donor (D) and electron acceptor (A) building units into D–A COF systems, where the D and A moieties form bicontinuous arrays of d-on-D and A-on-A units [72].

3.2 Imine-based COFs

Imine-based COFS can be synthesized through Schiff base reaction *via* co-condensation of aromatic amines and aldehydes in the presence of Lewis acid catalyst or an organic acid (**Fig. 2(c)**). In terms of their topologies, imine-based COFs could be classified into the five architectural groups: tetragonal, hexagonal, rhombic,

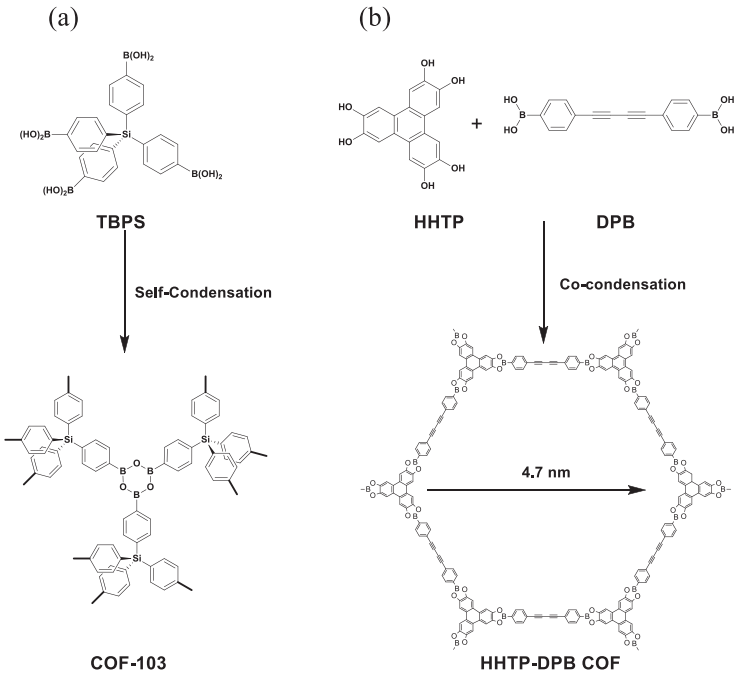

Fig. 3

Preparation of two boron-containing COFs. (a) Self-condensation of a monomer to construct 3D COF-103. (b) Co-condensation of DPB and HHTP monomers to synthesize 2D HHTP-DPB COF.

trigonal, and kagome structures. Many knots and linkers, as well as a battery of solvents, have been investigated. As the knot, the diverse array of π-units has been developed, including benzene, tetraphenylethene (TPE) triphenyltriazine, bicarbazole, triphenylbenzene, tetraphenylpyrene, tetrathiafulvalene (TTF), porphyrin, hexaazatriphenylene, hexaphenylbenzene, and hexabenzocoronene. Benzene, ortho-substituted benzenes, benzidine, triphenyl, bipyridine, and thiophene derivatives have been used as the linkers. The solvents that have been employed in the solvothermal syntheses have included 1,4-dioxane/mesitylene, o-dichlorobenzene (*o*-DCB)/*n*-butanol, ethanol, 1,4-dioxane/*o*-DCB, tetrahydrofuran (THF)/mesitylene, and dimethylacetamide/*o*-DCB [73–88]. Wang et al. prepared COF-LZU1 through co-condensation of 1,4-diaminobenzene and 1,3,5-triformylbenzene in 1,4-dioxane; it showed the catalytic activity in the Suzuki–Miyaura coupling reaction [73]. Imine-based COFs can display high potentiality and superiority in their structural regularity, and higher crystallinity when compared with boron-based COFs, as well as high chemical stability in organic solvents and water. These characteristics have made COFs useful materials for various applications [74,75]. For example, Chen et al. used the imine-based COFs TaDA and TaDAP and in studies of fluorescence and catalysis [76]. These COFs were constructed through condensations of 1,3,5-tris(4-aminophenyl)triazine with 1,3-benzenedialdehyde (TaDA) and 2,6-diformylpyridine (TaDAP) under solvothermal conditions. Interestingly, dispersions of both these COFs were strongly fluorescent, responding quickly to the presence of some metal ions; specifically, Fe^{3+} ions were detected by TaDAP with high sensitivity and selectivity. Furthermore, both COFs displayed excellent catalytic activity for the Knoevenagel reaction. Other applications for imine-based COFs include gas separation and storage, chemical sensing, energy storage, fluorescence, and drug delivery [77–84].

Although many knots are available for preparing 2D COFs, suitable monomers as nodes for 3D COFs remain mostly limited to tetra(4-aminophenyl)methane (TAPM) and 1,3,5,7-tetraaminoadamantane (TAA). For example, Yaghi et al. prepared the first imine-based 3D COF (COF-300) through co-condensation of TAPM and terephthalaldehyde [89]. This COF exhibited the 3D diamond-like structure and permanent porosity with the high surface area. Similarly, COF-320 [90], BF-COF-1, BF-COF-2 [91], LZU-301 [92], or 3D-Por-COF [93] have all been constructed from TAPM and TAA monomers. Moreover, a series of 3D salphen-based COFs and their metal-containing counterparts have also been prepared through the condensations of tetrakis(3-formyl-4-hydroxylphenyl)methane (TFHPM) with 4,5-dichlorophenylene-1,2-diamine (DCPDA) or 4,5-difluorophenylene-1,2-diamine (DFPDA) [61]. Recently, several 3D mesoporous COFs having the dia topology were synthesized from the tetrahedral knot TMSFTA and linear linkers based on 4,4′-diaminobiphenyl (DABP) and its derivatives [59].

3.3 Hydrazone-based COFs

Hydrazone-linked COFs have been prepared through co-condensation of aldehydes and hydrazides in presence of acetic acid as the catalyst (**Fig. 2(d)**). Integration of the ethoxy unit at the ortho position of the knot building units [such as 2,5-diethoxyterephthalohydrazide (DETH)] has been essential for forming hydrazine-linked COFs, inducing the formation of intramolecular hydrogen bonds. Subsequently, attempts have

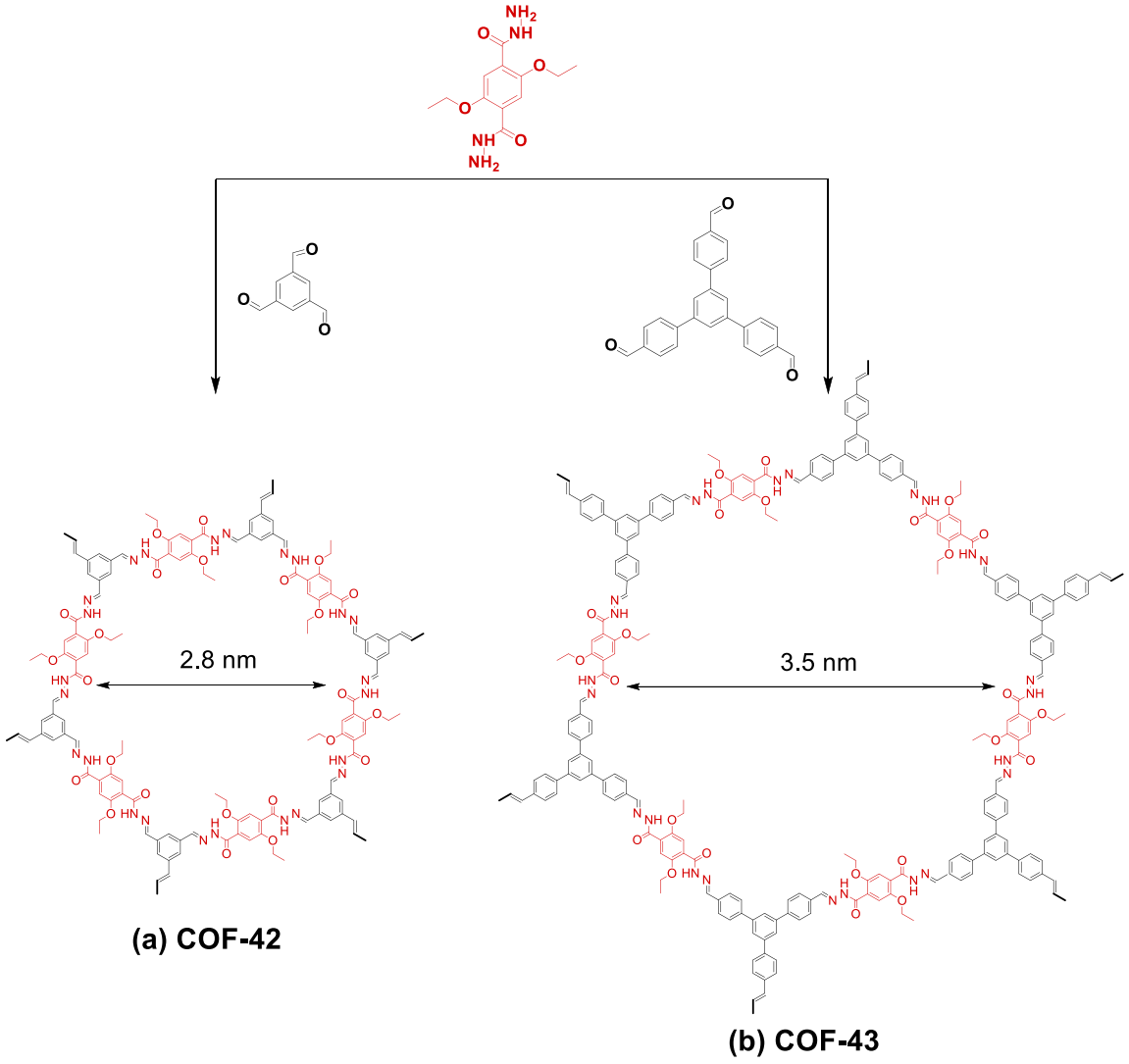

Fig. 4

Preparation of hydrazone-linked COFs of (a) COF-42 and (b) COF-43.

been made to secure the 2D conformation and enhance the crystallinity and chemical stability (**Fig. 4**). Various 2D COFs have been constructed using this strategy under solvothermal conditions. For example, the DETH building block has been employed with aromatic aldehydes to synthesize COF-42, COF-43 [94], and COF-JLU4 [95]. The TpODH COF has been synthesized from the aliphatic hydrazone linker oxalyldihydrazide (ODH) and TFP-3OHCHO in 1,4-dioxane/mesitylene, whereas TFTP-COF [96] and LZU-21 were obtained in mixtures of THF and mesitylene [34].

3.4 Azine-based COFs

Azine linkages ($-C=N-N=C-$) are present in a large number of COFs—the result of the short hydrazine monomer being used to connect two aldehydes and thereby form polygon skeletons having small pores. A variety of knots (*e.g.*, substituted benzenes, triphenylbenzene, triphenyltriazine, and pyrene) have been explored, leading to diverse topologies including hexagonal, trigonal, and rhombic COFs (**Fig. 5**) [97–102].

3.5 Imide-based COFs

Imide linkages can be formed through condensation of an amine with acetic anhydride at high temperature (up to 250 °C). The 2D polyimide (PI) COFs have been synthesized through reactions of aromatic dianhydrides and triamine building units, under the solvothermal condition in *N*-methyl-2-pyrrolidone/mesitylene mixtures with isoquinoline as catalyst [103]. The syntheses of PI-COF-1 or PI-COF-2 required heating at 200 °C for 5 days, while PI-COF-3 was formed at 250 °C over 7 days. Similarly, the 3D COFs of PI-COF-4 and PI-COF-5 were constructed at a lower temperature of 160 °C over 5 days. (**Fig. 6**) [104]. Moreover, COF-77 and COF-78 were synthesized at a low temperature of 85 °C within 3 days, under the solvothermal condition with the addition of trifluoroacetic acid (TFA) as catalyst [105]. Other synthetic methods that have been deployed for the formation of imide-

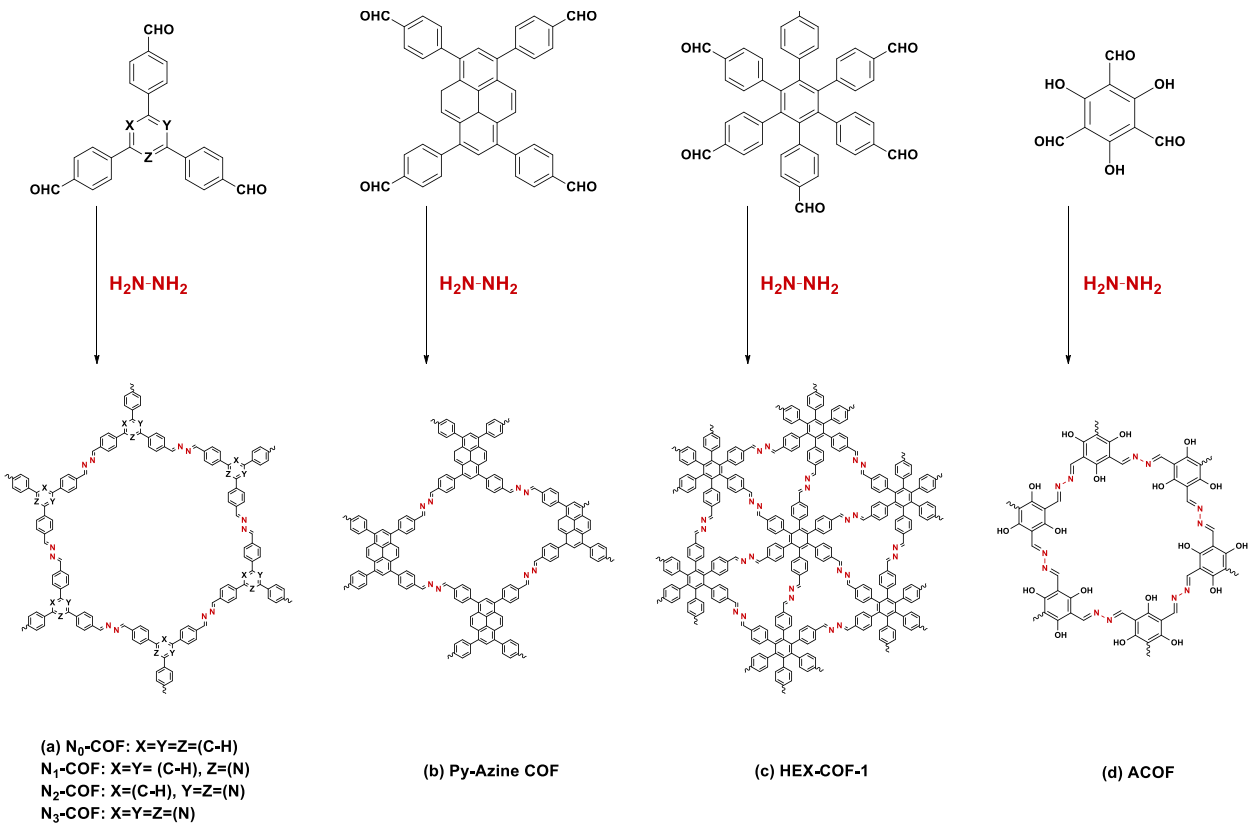

Fig. 5

Preparation of azine-linked COFs: (a) N_x-COFs ($x = 0$, 1, 2, and 3), (b) Py-Azine COF, (c) HEX-COF-1, and (d) ACOF.

linked COFs include ionothermal and catalyst- and solvent-free methods [106-108].

3.6 Ketoenamine-based COFs

Ketoenamine-based COFs have been prepared by Banerjee et al. through irreversible enol–keto tautomerization of ketenimine linkages in imine-based COFs (**Figs. 2(f) and 2(g)**). The building block used to synthesize the imine-based COF was Tp, which features an OH group adjacent to a CHO group (**Figs. 7(a) and 7(b)**). Ketoenamine COFs have displayed excellent chemical stability against strong bases—a characteristic that is highly useful for many applications. Nevertheless, the irreversibility of the enol–keto tautomerization in the preparation of these COFs hinders error-correction in the COF lattice, thereby decreasing their crystallinity [33]. Recently, we reported [109] β-ketoenamine–linked COFs displaying excellent CO_2 adsorption capability and high performance supercapacitance; we investigated the role of the monomer's planarity on the properties of these COFs. We constructed three β-ketoenamine–linked COFs through solvothermal Schiff-base [3 + 3] polycondensations of TFP-3OHCHO with three different tris(aminophenyl) derivatives exhibiting different degrees of planarity, with carbazole, amino, and pyridine groups, respectively (**Figs. 7(c)–(e)**). The TFP-COFs displayed high specific surface areas (686 $m^2\ g^{-1}$) and good crystallinity. Moreover, these TFP-COFs displayed high CO_2 uptake efficiencies (200 mg g^{-1} at 273 K), as well as excellent electrochemical specific capacitances (291.1 F g^{-1}). This exceptional performance as supercapacitors and for gas storage arose from their conjugated enamine structures featuring redox-active triphenyl carbazole, amino, and pyridine groups. Monomers of higher planarity resulted in COFs having stronger quadrupolar interactions with the guest CO_2 molecule. β-Ketoenamine–linked COFs have also been used in a diverse array of applications, including gas separation and storage, and chemical sensing [110–112].

3.7 sp^2-Hybridized-carbon-conjugated COFs

The synthesis of fully π-conjugated COFs became accessible through Knoevenagel condensations of benzyl cyanides and aldehydes in the presence of the base catalyst. Jiang et al. proposed the first $C=C$-linked COF (sp^2c-COF) through the condensation of 1,4-phenylenediacetonitrile and tetrakis(4-formylphenyl)pyrene (TFPPy) in 1,4-dioxane/mesitylene mixtures in the presence of aqueous NaOH (4 M) as the catalyst [113]. Similarly, various sp^2c-COFs has also been synthesized through reactions of TFPPy with linkers of various lengths (**Fig. 8**) [114]. A 2D poly(phenylenevinylene) framework (2DPPV) has been prepared through the condensation of the three-armed aromatic aldehyde 1,3,5-tri(4-formylphenyl)benzene and 1,4-phenylenediacetonitrile in *o*-DCB containing cesium carbonate as the catalyst [115]. A 2D porphyrin-based sp^2-hybridized-carbon-conjugated COF (Por-sp^2c-COF) has been synthesized

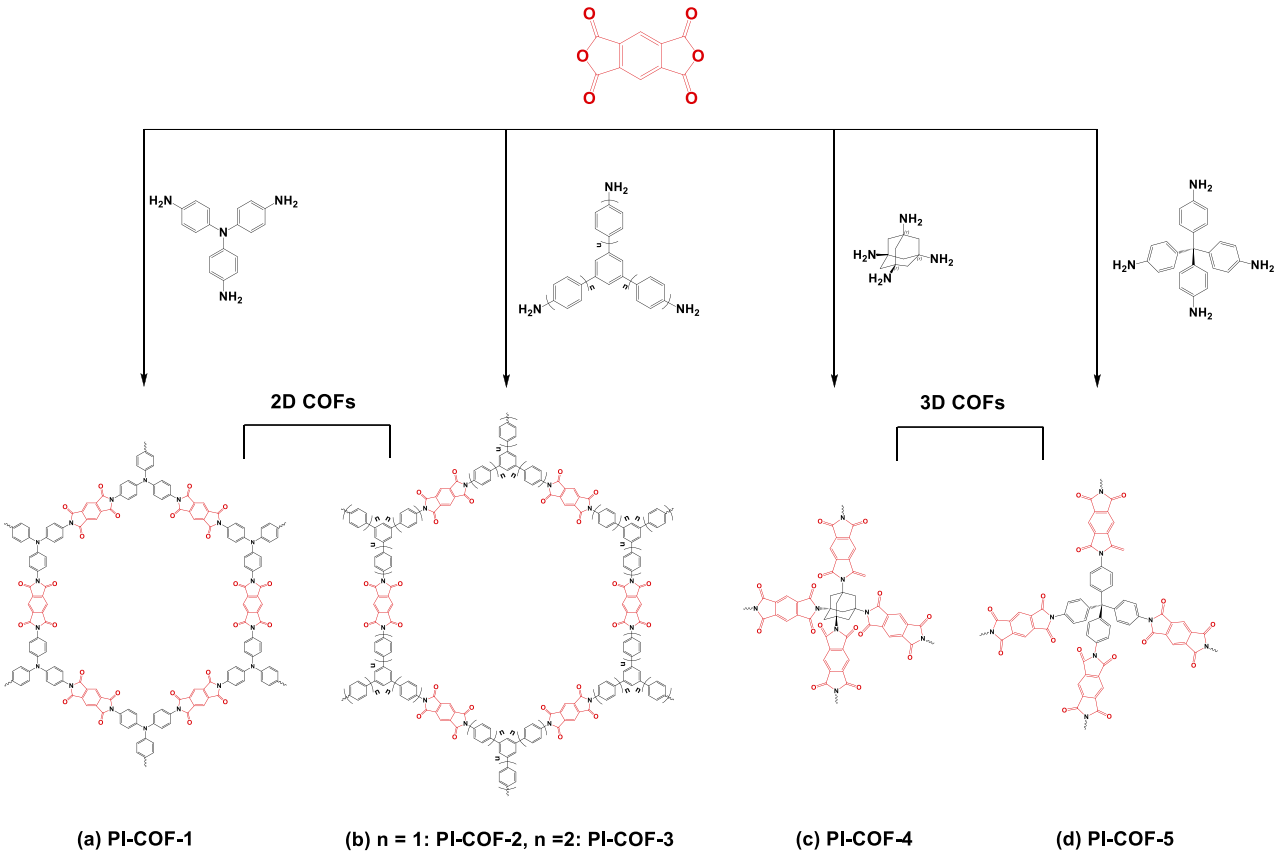

Fig. 6

Preparation of imide-linked COFs: (a) PI-COF-1, (b) PI-COF-2 and PI-COF-3, (c) PI-COF-4, and (d) PI-COF-5.

[116] and the 2D TP-COF, featuring triazine central planar units bridged by sp^2-hybridized carbon linkers, was constructed in a mixture of 1,4-dioxane and $CHCl_3$ [117]. The unsubstituted olefin-linked COF-701 was prepared through aldol condensation of 2,4,6-trimethyl-1,3,5-triazine and 4,4′-biphenyldicarbaldehyde in mesitylene/dioxane/acetonitrile mixture, catalyzed by TFA [118]. Various olefin-linked hexagonal COFs—g-$C_{31}N_3$, g-$C_{37}N_3$, and g-$C_{40}N_3$–COF—has prepared through condensations of 3,5-dicyano-2,4,6-trimethylpyridine with 4,4′-diformyl-1,1′-biphenyl, 1,3,5-tris(4-formylphenyl)benzene, and 4,4′′-diformyl-*p*-terphenyl, respectively, catalyzed by piperidine in anhydrous DMF [119].

3.8 Other linkages

Several other linkages have been used to prepare COFs, in addition to the more common ones discussed above. Yaghi et al. constructed the 3D material COF-202 featuring strong covalent borosilicate bonds (B–O, Si–O) linking tetrahedral and triangular building units to form the structure similar to the topology of carbon nitride (**Fig. 2**). COF-202 displayed high porosity, surface area and thermal stability [120]. Moreover, Valtchev et al. synthesized polyarylether-based COFs (PAE-COFs) through nucleophilic aromatic substitution of *o*-difluorobenzene and catechol building blocks, forming ether linkages. The PAE-COFs displayed great stability against harsh chemical environments, including strong acids and bases, boiling water, and oxidative and reductive conditions [121]. Li et al. constructed a new 2D conjugated COF films linked by $C-C$ bonds via Suzuki polymerization. The reaction was carried on a water-toluene interface providing a large thin film sheet [122]. Wang et al. prepared an aryl ether (ArOAr)–based COF through solvothermal condensation of trinitrophenol and 2,4,6-trihydroxypyrimidine; it exhibited the maximum specific capacitance of 133 F g^{-1} at 0.3 A g^{-1} [123]. Moreover, Thomas et al. prepared triazine-based COFs (CTFs) through ionothermal cyclotrimerization of nitrile building units in the presence of molten $ZnCl_2$ at 400 °C [124]. For example, CTF-1 exhibited a hexagonal structure with the pore size of 1.2 nm, extended in 1D channels, and the surface area of 791 m^2 g^{-1}. CTFs could possess high surface areas, thermal and chemical stabilities with wide range of applications in, for example, heterogeneous catalysis, electrocatalysis, and energy storage [125–130]. Recently, we subjected both triazine-based trifunctionalized phenolic and amine linkers to a Mannich reaction with paraformaldehyde to synthesize a covalent benzoxazine framework (CBF). Thermal curing of this CBF yielded the highly cross-linked CBF. Subsequent carbonization and KOH activation provided the N-atom-doped microporous carbon (N-DMC, **Fig. 9**). This N-DMC displayed excellent CO_2 capture capacities (up to 7.46 $mmol^{-1}$ at 273 K) as well as an excellent electrochemical capacitance of 185 F g^{-1} [42].

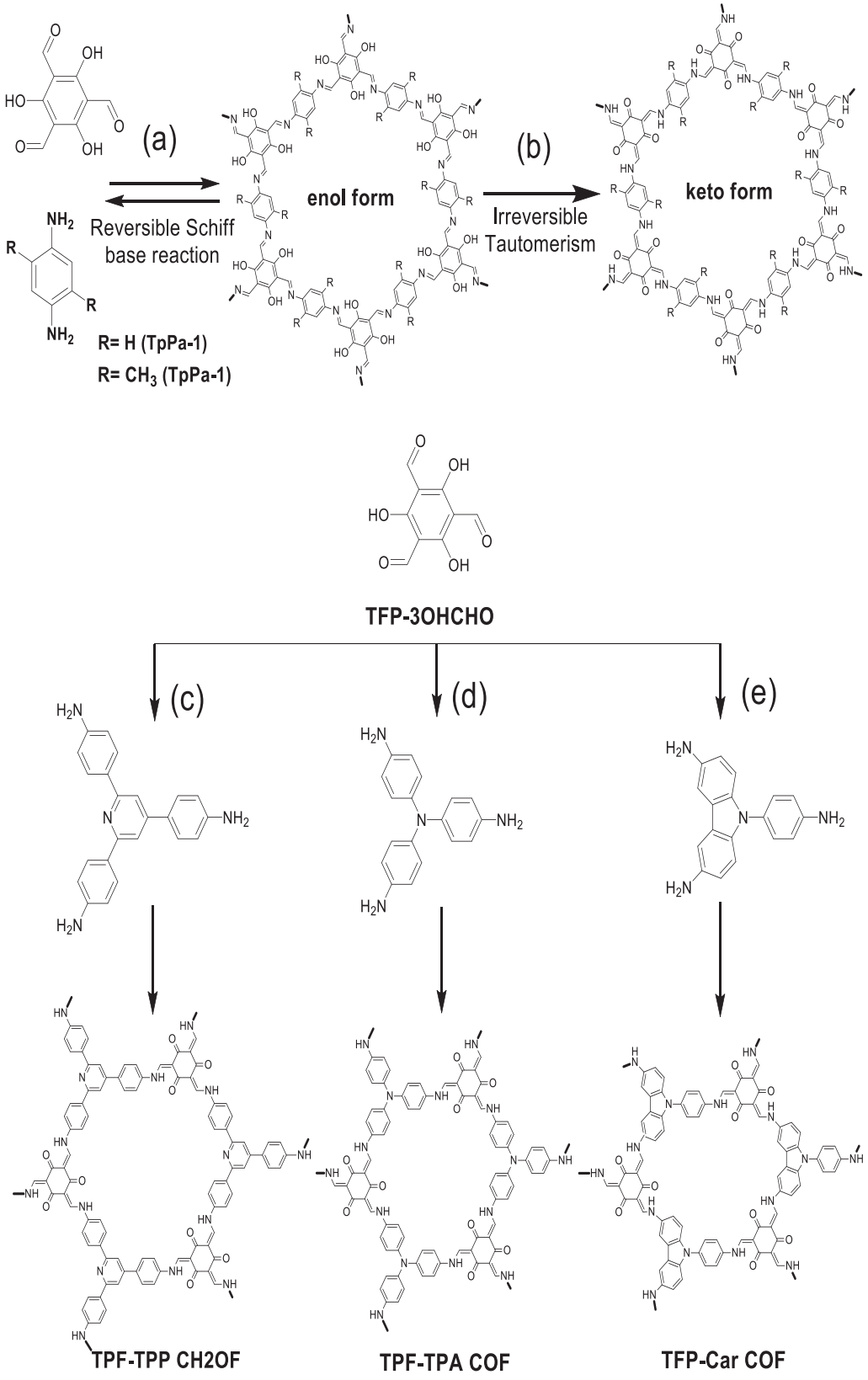

Fig. 7

(a, b) Representation of two-step syntheses of three β-ketoenamine–linked COFs from TpPa-1 and TpPa-2 through (a) reversible Schiff base formation and (b) irreversible enol-to-keto tautomerization. (c–e) Preparation of the β-ketoenamine–linked COFs (c) TFP-TPP, (d) TFP-TPA, and (e) TFP-Car from TFP-3OHCHO and tris(aminophenyl) derivatives having different degrees of planarity.

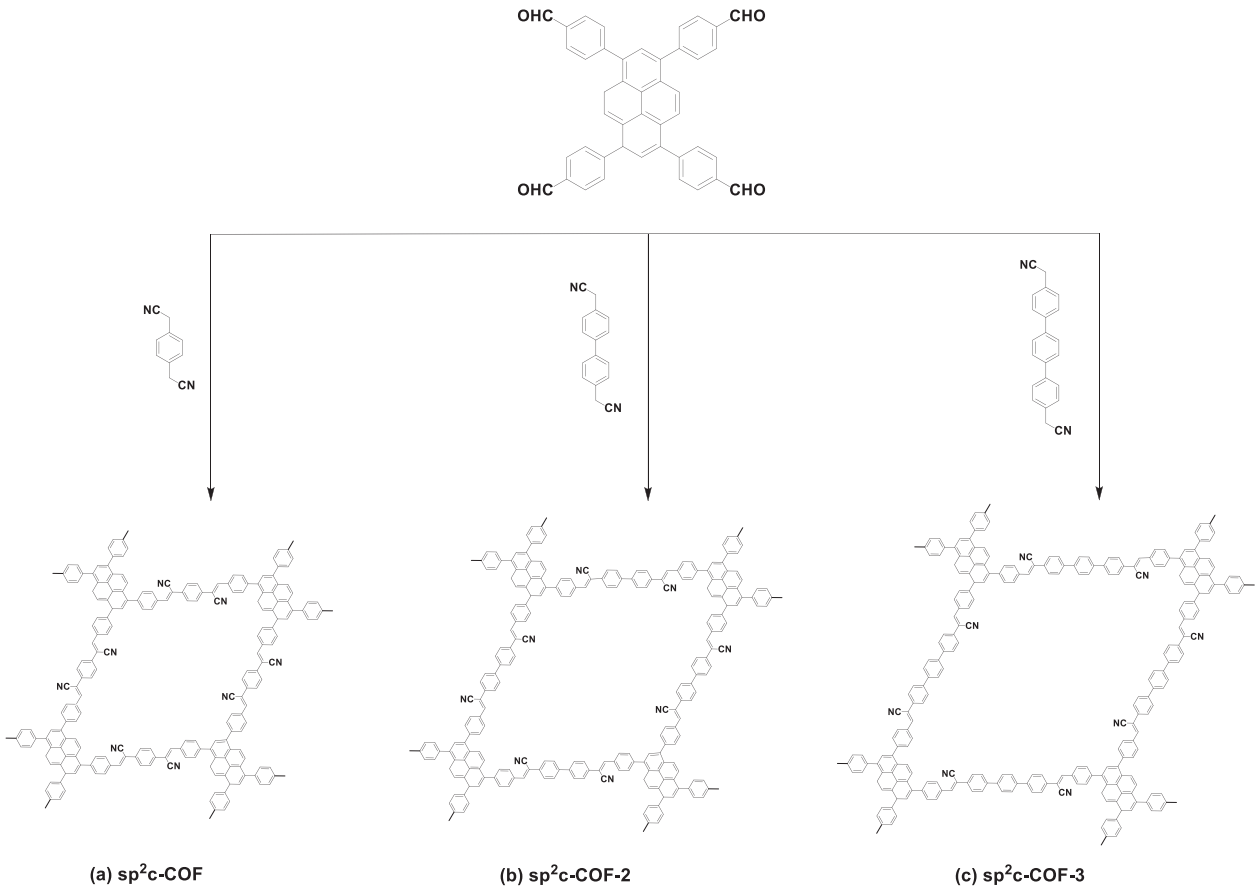

Fig. 8

Preparation of (*C* = *C*)-linked COFs: (a) sp^2c-COF, (b) sp^2c-COF-2, and (c) sp^2c-COF-3.

3.9 Dual linkages

In addition to the single-linkage COFs strategies mentioned above, the development of COFs with dual-linkages has also been explored (**Fig. 10**). For example, 4-formylphenyl boronic acid (FPBA) was a typical monomer possessing bifunctional reactive sites; it forms boronate esters with imine linkages, boroxines with imine linkages, and boronate esters with hydrazone linkages, resulting in hexagonal rhombic and tetragonal topologies [131–133]. Chen et al. employed a double-stage strategy to prepare the HHTP-FPBA-TATTA COF through condensation of two C_3-symmetric monomers—4,4′,4″-(1,3,5-triazine-2,4,6-triyl)trianiline (TATTA) and 2,3,6,7,10,11-hexahydroxytriphenylene (HHTP)—with the bifunctionalized monomer FPBA [131], while the condensation of HHTP and FPBA with 1,3,5-tris(4-aminophenyl)benzene (TAPB) provided a 2D COF (**Fig. 10(a)**) [132]. Two other 3D COFs have also been synthesized from dual monomers (imine and boroxine) using the same strategy (**Fig. 10(b)**) [133].

4 Synthetic methods

Finding suitable conditions for the synthesis of COFs is crucial if they are to be used in real-world applications. In addition to solvothermal methods, which are used commonly to synthesize COFs, many other methods have been developed [134]. Here, we summarize the methods that have been used to construct COFs, including solvothermal, ionothermal, microwave-assisted, sonochemical, mechanochemical, and light-induced processes (**Fig. 11**).

4.1 Solvothermal synthesis

Similar to the typical syntheses of inorganic zeolites performed in autoclaves, several COFs have been obtained using solvothermal methods [135]. A typical process involves heating a mixture of monomers, dissolved in a combination of carefully chosen solvents, at 80–120 °C in a sealed Pyrex tube for 3–7 days. The choice of solvent is crucial to enhance the solubility of the monomers. Solvent mixtures (*e.g.*, 1,4-dioxane/mesitylene) can be used to mediate the diffusion of the monomers into the solution, thereby accelerating the nucleation of COFs. Moreover, the sealed environment ensures that water is available during the reaction, thereby improving the crystalline growth of the COFs [136]. The first COFs synthesized using this method (COF-1 and COF-5) were reported by Yaghi et al. [23]. COF-1 was assembled through self-condensation of 1,4-benzenediboronic acid (BDBA); it exhibited the layered hexagonal framework. Similarly, COF-5 was prepared through condensation of BDBA and HHTP; it had the coplanar

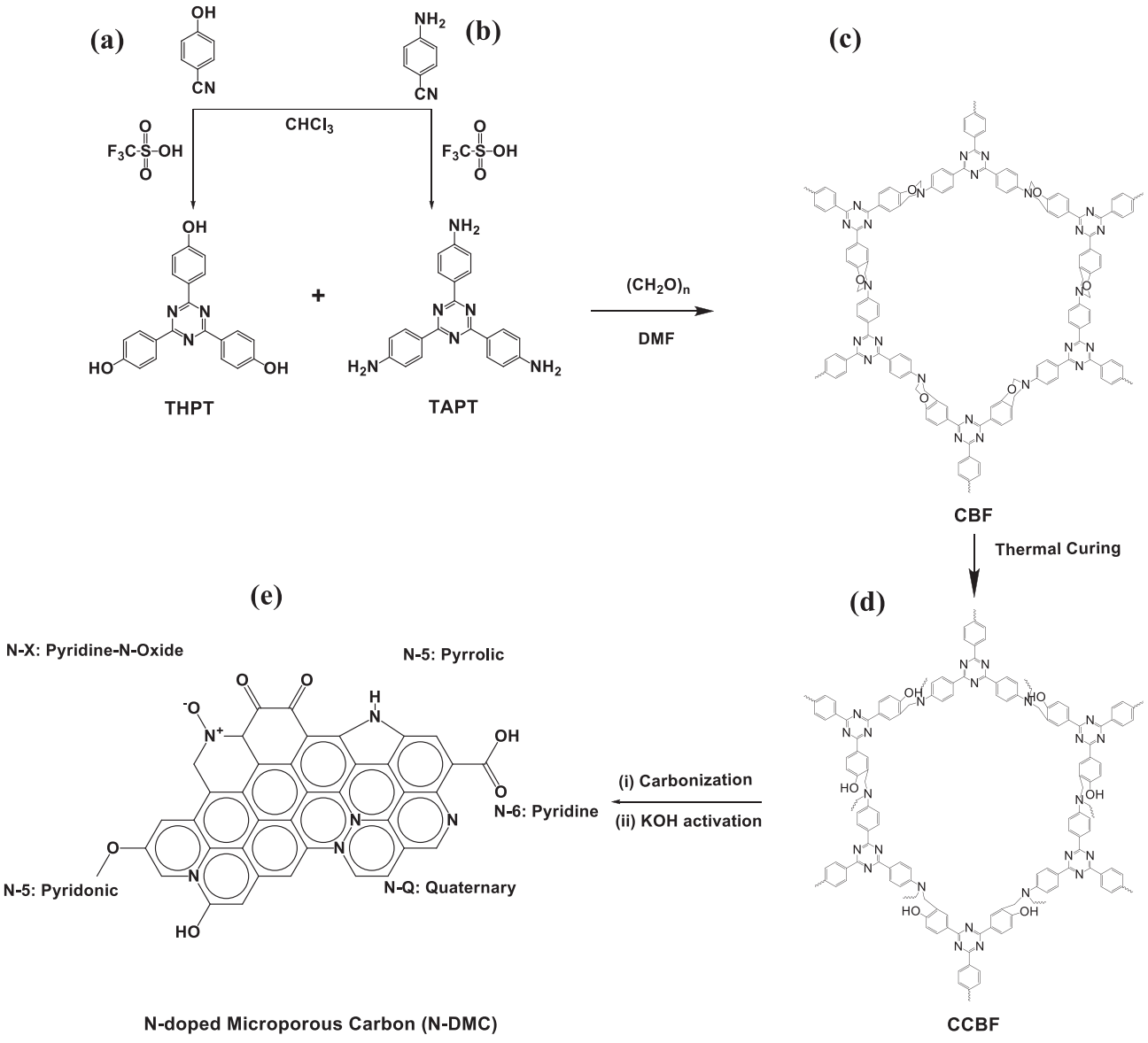

Fig. 9

Synthesis of the trifunctionalized phenolic and amine monomers: (a) THPT and (b) TAPT; their Mannich reaction to give (c) CBF; followed by thermal curing to form (d) CCBF, and carbonization and activation with KOH to give (e) N-DMC.

extended sheet structure. The majority of COFs prepared using solvothermal methods have been insoluble and unprocessable powders, potentially limiting their applications. Dichtel et al. used a solvothermal route to prepare 2D COF films on the single-layer graphene; this method would be beneficial in the preparation of organic electronic device, where the thin-film formation is essential for enhancing the optoelectronic property [137]. Some other 2D COF films possessing unique properties have also been synthesized using this method [138].

4.2 Ionothermal synthesis

In the ionothermal method, a molten salt or an ionic liquid is used as both the solvent and catalyst to form solids at high temperature (*ca*. 400 °C) and pressure [124]. This method was used by Thomas et al. to synthesize porous crystalline COFs through cyclization and trimerization of nitrile structural units in molten $ZnCl_2$ at 400 °C; these CTFs displayed high crystallinity, high chemical and thermal stabilities [124,139]. Nevertheless, the harsh conditions required for this method decrease its popularity, because they narrow the scope of available building blocks and can also result in undesirable decomposition and side reactions, thereby limiting its applicability. Recently, Qiu et al. developed an ambient-temperature-and-pressure ionothermal technique to synthesize 3D COFs (3D-IL-COFs). They used 1–butyl–3-methylimidazolium bis((trifluoromethyl)sulfonyl)imide, a liquid at room temperature, as both the solvent and catalyst for Schiff base formation (**Fig. 12**). These 3D-IL-COFs formed within a significantly shorter reaction time (12 h) when compared with the times required for traditional solvothermal methods (3–7 days) [140].

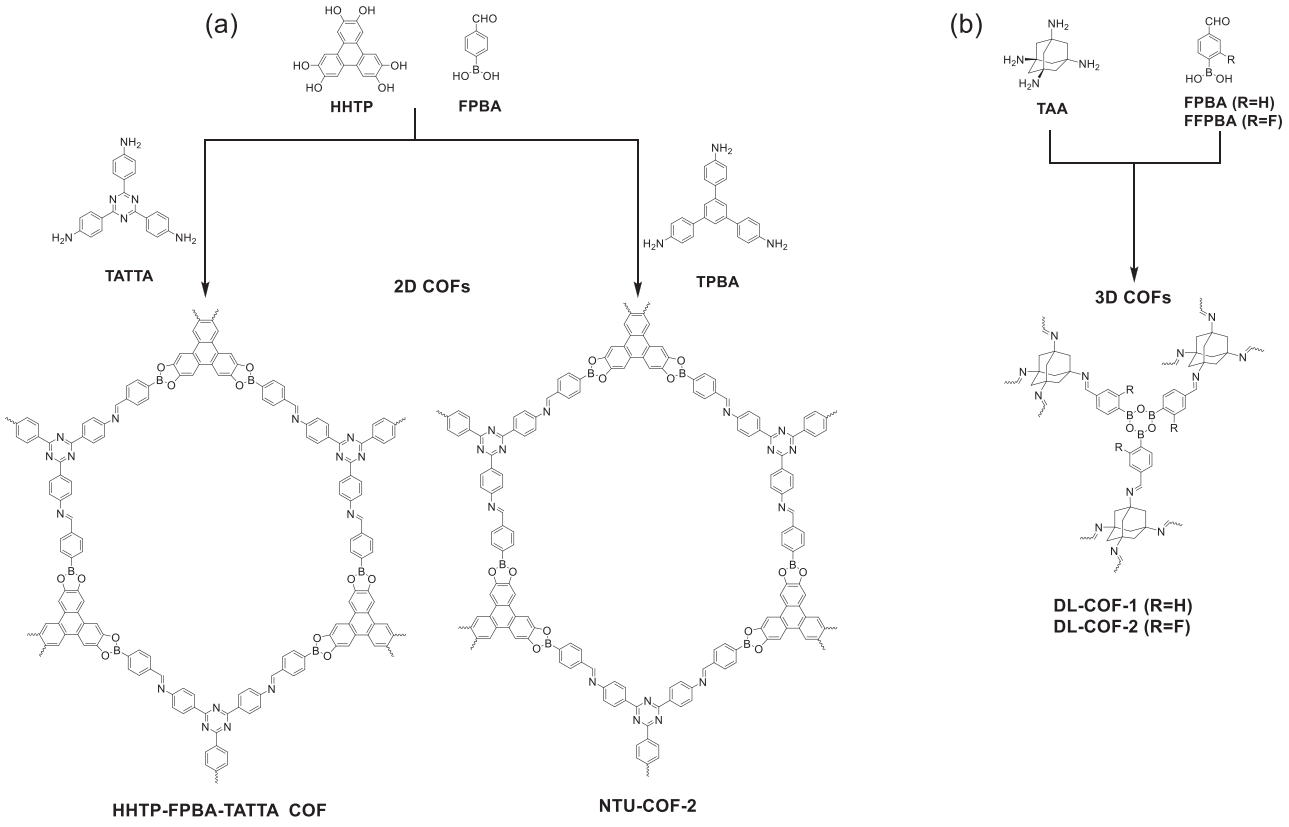

Fig. 10

Synthesis of 2D COFs (a) and 3D COFs (b) using dual linkers.

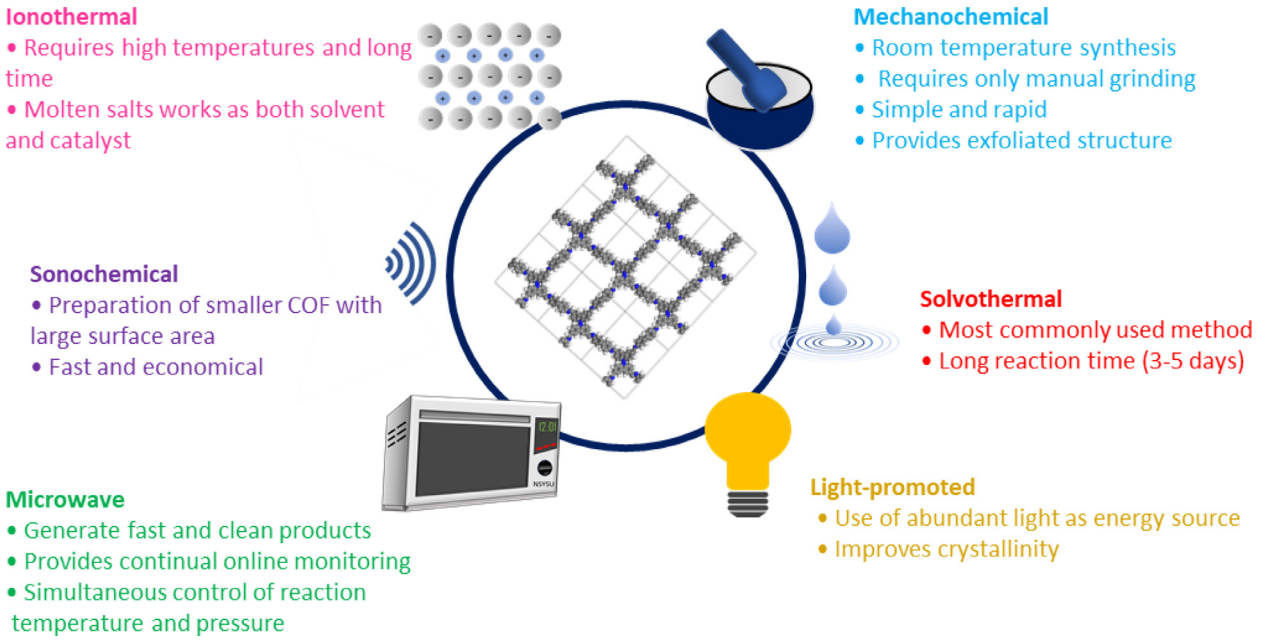

Fig. 11

Schematic representation of the properties and advantages of various synthetic routes toward COFs.

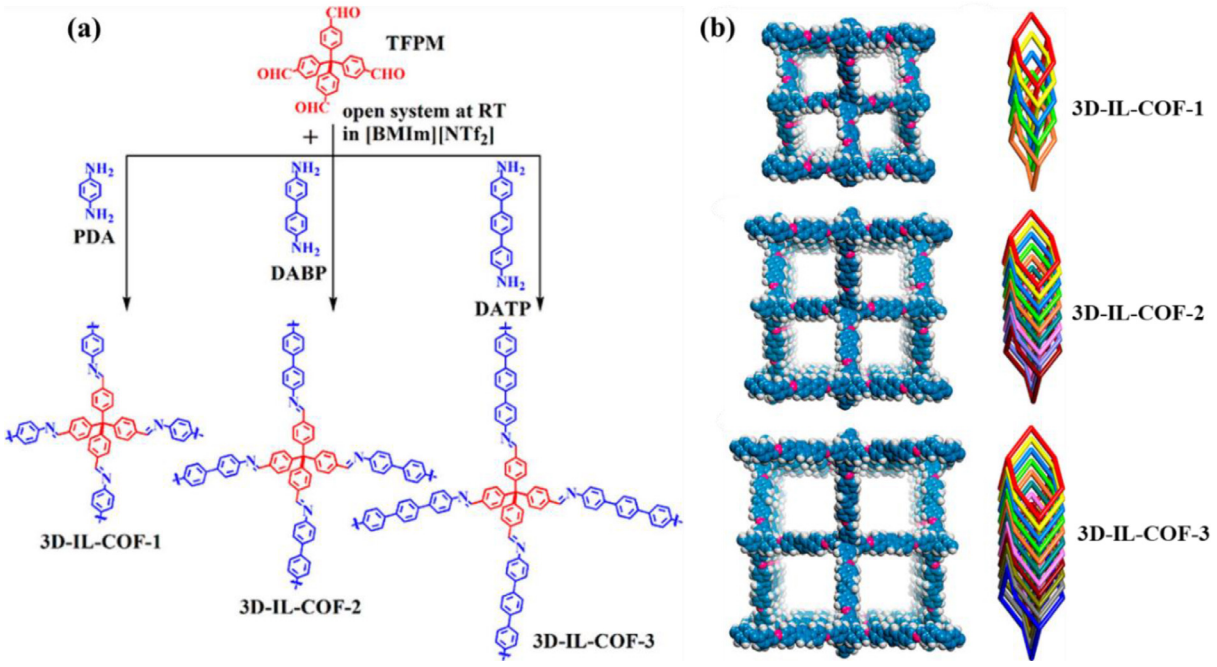

Fig. 12

(a) Schematic and (b) structural representations of the synthesis of 3D-IL-COFs through the ionothermal method at ambient temperature and pressure. C, blue; H, gray; N, red. (Adapted from Ref. [131] with permission; copyright 2018, American Chemical Society.

4.3 Microwave synthesis

Microwave irradiation has been explored widely as an alternative method for the synthesis of COFs [141]. It has many advantages over the solvothermal method, including shorter reaction times and cleaner products, as well as the ability to monitor the phase behavior and simultaneously control the temperature and pressure [142]. Recently, Cooper et al. synthesized COF-5 through microwave irradiation with stirring at 100 °C at a power of 200 W for 20 min [143,144]; this synthetic route was 200 times faster than the reported solvothermal synthesis, which required 72 h [23]. Moreover, microwave-assisted synthesis enhanced the surface area of COF-5 by removing impurities; its BET surface area [$S_{BET(microwave)} = 2019\ m^2\ g^{-1}$] was higher than that of the corresponding material prepared using the solvothermal method [$S_{BET\ (solvothermal)} = 1590\ m^2\ g^{-1}$]. The extraction of impurities from this material was achieved by heating the gray precipitate of isolated COF-5, which had formed in the reaction vessel, with dry acetone at 55 °C for 20 min at 200 W. This process was repeated twice to remove the purple color of the supernatant, arising from the formation of an oxidized form of HHTP.

4.4 Sonochemical synthesis

Sonochemical synthesis can be a favored alternative to conventional methods because of its rapidity and economy [145]. In this method, ultrasound induces bubbles in the solvent; they grow and collapse in the phenomenon known as cavitation, providing to extremely high local pressure and temperature, thereby initiating and accelerating chemical reactions. Ahn et al. used this approach to prepare COF-1 and COF-5 within a short reaction time of 1 h [146]. The time required to synthesize COF-1 was 400 times shorter than the conventional method, and this sonochemical approach increased the reaction batch size up to 0.5 L and resulted in a high surface area of 2122 $m^2\ g^{-1}$. Using this mild method, Shim et al. synthesized COF-5 on the surfaces of carbon nanotubes and graphene to provide core/shell structures [147].

4.5 Mechanochemical (MC) synthesis

The MC route, using only a pestle and mortar to perform manual grinding, is gaining considerable attention because it is simple, rapid, solvent-free, and environmentally friendly method performed at room temperature [148,149]. Banerjee et al. proposed the solvent-free and rapid MC syntheses of the COFs through Schiff base condensations at room temperature using a manual grinding setup with a mortar and pestle [150]. The change in color that occurred during grinding indicated the formation of COFs (**Fig. 13**). Moreover, the exfoliation of the COF layers during the MC synthesis caused the COFs to form the graphene-like layered structures, which is different of the COFs prepared solvothermally. Recently, Wang et al. used the same method to synthesize the COF TpAzo within a short time (20 min) through condensation of 4,4-azodianiline and Tp; this COF had the sheet-like morphology, high thermal stability and porosity [151].

4.6 Light-induced synthesis

A new highly conjugated and crystalline COF was constructed under the simulated sunlight irradiation at wavelengths of 200–2500 nm in the presence of a co-catalyst. A mixture of hexaketocyclohexane octahydrate (HCH) and 1,2,4,5-benzenetetramine tetrahydrochloride (BTA) was dissolved in

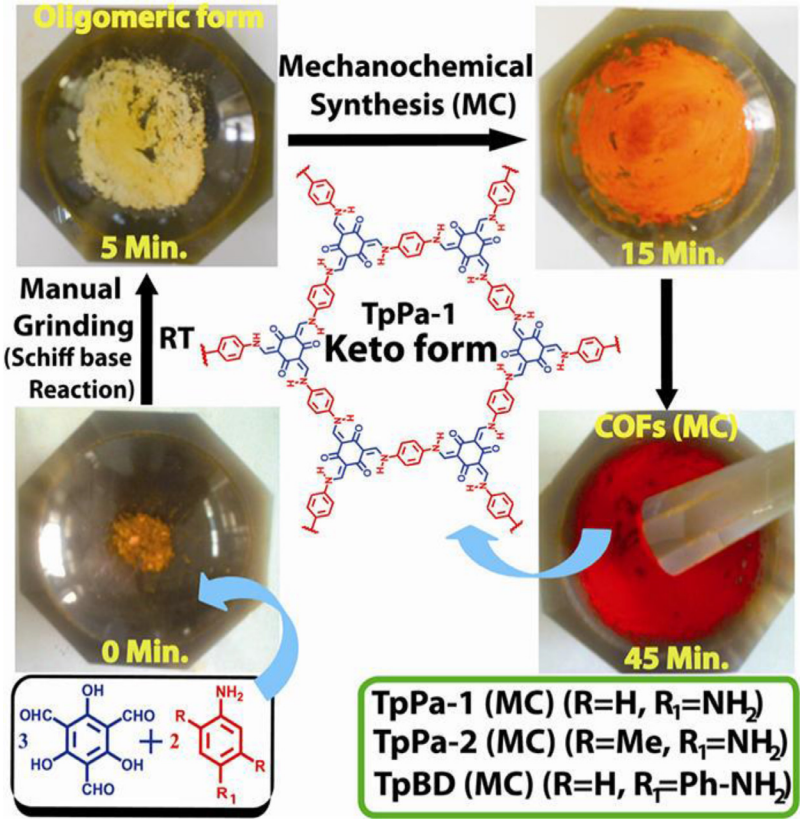

Fig. 13

MC syntheses of TpPa-1, TpPa-2, and TpBD in the mortar and pestle. (Reproduced from Ref. [150] with permission; copyright 2013, American Chemical Society).

a mixed solvent under an inert atmosphere; a co-catalyst (acetic acid and water) was added to the mixture to induce condensation. An amorphous version of hcc-COF was obtained in the absence of light. The crystalline hcc-COF exhibited high electrical conductivity (2.22×10^{-3} S m^{-1}), presumably because of the formation of an extended conjugated structure that enhanced charge transfer [152].

4.7 Other methods

The comparison of the advantages and disadvantages of the synthesis strategies of COFs was summarized in Table 1. In addition, using the magnetic properties of nanoparticles is a cost-effective, low-toxicity method for the synthesis of COFs. Cai et al. prepared the bouquet-shaped magnetic porous nanocomposite through the grafting of the COF onto amino-functionalized Fe_3O_4 nanoparticles [153]. Similarly, a general two-step approach—combining MC grinding and crystallization—has been used to obtain a magnetic COF composite [154]. Recently, Yan et al. reported the facile solution-phase method for the synthesis of spherical imine-based COFs at room temperature and ambient pressure. If it could be generalized, the simplicity of this approach suggests that it would be a promising method for bulk production [155].

5 Applications

Advancements in COF research have enabled studies of their many applications. Applying the design principles in **Section 2** and using the variety of linking types discussed in **Section 3**, it becomes possible to construct a diverse range of functional COFs to satisfy the criteria required for many applications. In this Section, we summarize four applications in which COF materials have served as platforms: CO_2 storage, catalysis, supercapacitors, and photovoltaics.

5.1 Carbon dioxide storage

Global warming caused by elevated levels of atmospheric CO_2 is a major concern that has encouraged the development of CO_2 capture tools [156]. Several types of porous materials have been explored for CO_2 storage, including porous carbons, zeolitic imidazolate frameworks (ZIFs), MOFs, and COFs; their CO_2 capture has typically been measured at temperatures of 273 and 298 K and under a pressure of 1 bar (**Table 2**). Recently, we prepared triphenylamine (TPA) or triphenyltriazine (TPT)-based COFs through the polycondensations of tris(4-aminophenyl)amine or 2,4,6-tris(4-aminophenyl)triazine, respectively, with various triarylaldehydes with different planarities, symmetries, and N-atom contents (**Fig. 14**). The degrees of crystallinity and surface areas of the resultant COFs were highly influneced by the symmetry and planarity of the monomers. Furthermore, the incorporation of higher-N-content triaryltriazine and more planar units into the TPA or TPT-COFs backbones could enhance their interactions with CO_2 [40]. Moreover, various 3D COFs with different structures have been utilized as scaffold for carbon dioxide adsorption. For example,

Table 1

Comparison of the advantages and disadvantages of the synthesis strategies of COFs.

Methods	Advantages	Disadvantage
Solvothermal		
	• Widely used methods due to the simplicity and providing high crystalline products, with almost 100% defects healing • A large combination of solvents can be used	• Products are insoluble and unprocessable powders, which potentially limiting their applications • Long reaction time (3–5 days) • Can not be used for insoluble building blocks
Ionothermal		
	• Significantly shorter reaction time (12 h) when compared with the times required for traditional solvothermal methods (3–7 days)	• Require high temperature • Undesirable decomposition and side reactions
Microwave		
	• Generate fast and clean products • The ability to monitor the phase behavior • Simultaneous control of reaction temperature and pressure	• Not as simple as other methods
Sonochemical		
	• Rapid and economic • Increased the reaction batch size up to 0.5 L	• Only applicable for small COFs
Mechanochemical		
	• Room temperature synthesis • Requires only manual grinding • Simple, rapid, solvent-free, and environmentally friendly synthesis • •Provide exfoliated structure	• Only applicable for small building blocks. • Does not have a medium for orientation and crystalline arrangements.
Light-induced		
	• Use of abundant light as energy source • Simple and solvent-free • Improved crystallinity	• Limited to synthesis of conjugated COFs structures

Table 2

CO_2 capture properties of bicarbazole-based COFs and other porous materials.

Material	Covalent bond type	Adsorption at 273 K (mg g^{-1}) at 1 bar	Adsorption at 298 K (mg g^{-1}) at 1 bar	Surface area (m^2 g^{-1})	Q_{st} (KJ mol^{-1})	Pore volume cm^3 g^{-1}	Ref.
TDCOF-5	Boronate	92.4		2497	21.8	1.3	[158]
CTF-1	Triazine	108		415	31		[159]
CTF-CSU1	Triazine	151		685			[160]
cCTF-500	Triazine	133	80	1247	43	1.04	[161]
TpPa-1	ketoenamine	153		535			[28]
2,3-DhaTph	imine	84		1019		2	[162]
Cz-BD COF	Imine	126	66	2111	27.8	1.061	[48]
(HO)100%-H2P-COF	Imine	63	35	1284	36.4	1.02	[163]
(AcOH)50%-H2P-COF	Imine	117	64	866	17.8	0.45	[164]
TPA-COF-3	Imine	91.15	63.94	557	28.11	0.353	[40]
ZIF-8–90		5.22	2.37	949		0.572	[165]
GOF		–	218.68	506			[166]
N-DMC		–	124.8	1866			[167]
An–COP-2	Triazine	61.6	66.8	1130		1.02	[168]
VFBZ-CN	Triazine	151	300	560		1.25	[169]

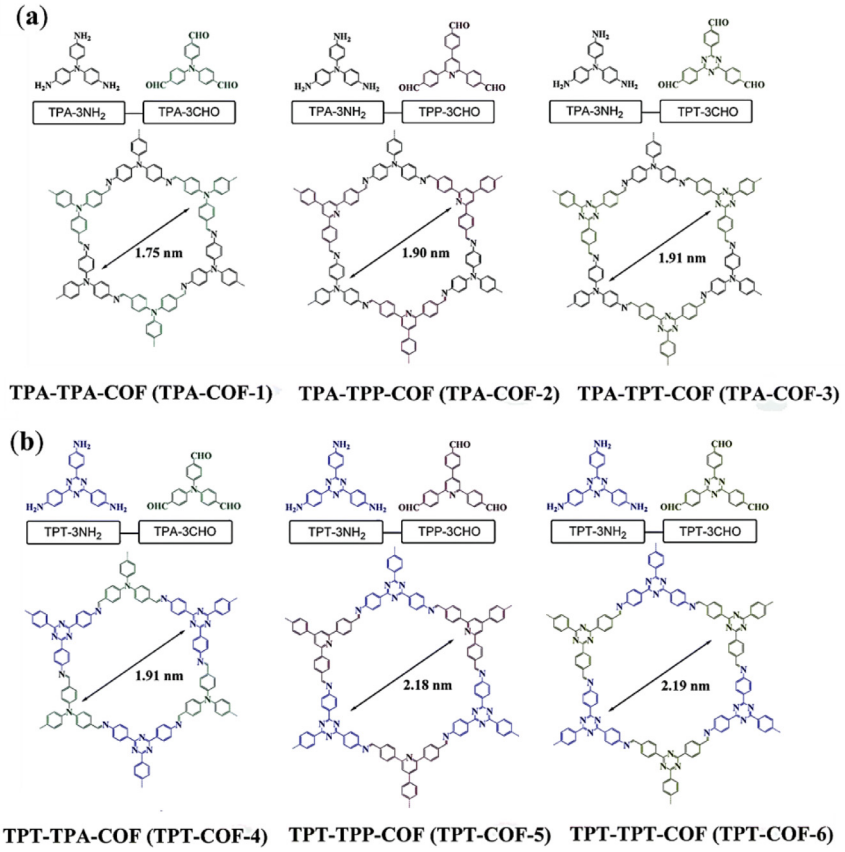

Fig. 14

Syntheses of (a) three TPA-COFs from triphenylamine and three aldehydes and (b) three TPT-COFs from triphenyl triazine and three aldehyde monomers of various planarities.

Yaghi et al. have synthesized a series of COFs for CO2 storage, among them 3D COF-102 and COF-103 featured a high surface area of 3620 and 3530 m^2/g and outstanding carbon dioxide uptake up to 1200 and 1190 mg/g at 50 bar and 298 K [157].

5.2 Catalysis

Functional porous materials having high surface areas have been used widely for heterogeneous catalysis [170]. For example, zeolites are powerful catalysts in the refining and petrochemical industries [171]. Motivated by developments in the use of hybrid crystalline MOFs for catalysis [172,173], COFs have recently become candidates for efficient and robust catalysis because they often feature catalytic sites and stability toward thermal treatment, water, and organic solvents. Wang et al. were the first to use COFs as efficient catalysts (**Fig. 15**) [73]. Their imine-linked COF material COF-LZU1, obtained through Schiff base formation from 1,4-diaminobenzene and 1,3,5-triformylbenzene, featured a 2D eclipsed layer sheet topology, which decreased the distance between the N atoms in the adjacent layers to 3.7 Å, suggesting a suitability for this COF to strongly coordinate metal ions. Post-treatment with $Pd(OAc)_2$ at room temperature provided the composite Pd/COF-LZU1, which they tested as a catalyst for the Suzuki–Miyaura coupling with a broad scope of reactants. This catalyst provided high yields of products (96–98%) with high stability and ease of recyclability. Furthermore, the unique structure of this composite provided superior catalytic activity when compared with Pd-containing MOFs—in terms of lower catalyst loadings, shorter reaction times, and higher product yields. Pd/COF-LZU1 is distinguished by its stacked layers in a sheet arrangement, and the short distance between N atoms in the adjacent layers, providing a strong scaffold for the incorporation of catalytic sites. Moreover, its extended channels ensured efficient access to these active sites and rapid diffusion of reactants and products from the COF surface.

5.3 Supercapacitors

COFs can function as platforms for electrical double-layer supercapacitors (EDLC) because of their high surface areas [174,175]. Dichtel et al. were the first to report the use of 2D COFs as pseudocapacitors [71]. They condensed 2,6-diaminoanthraquinone (DAAQ), as a redox-active unit, with TFP-3OHCHO under solvothermal conditions (**Fig. 16**). The resultant DAAQ-TFP COF exhibited the high surface area (1280 $m^2\ g^{-1}$) and highly ordered porosity—characteristics favorable for charge transfer from the redox-active units of COFs to the surface of the electrodes of the supercapacitor. Electrochemical measurement revealed that the capacitance of the electrode was stable at 40 $F\ g^{-1}$ over 5000 charge/discharge cycles. This low capacitance indicated that only 2.5% of the redox-active moieties of the DAAQ units were electrochemically accessible, due to the random

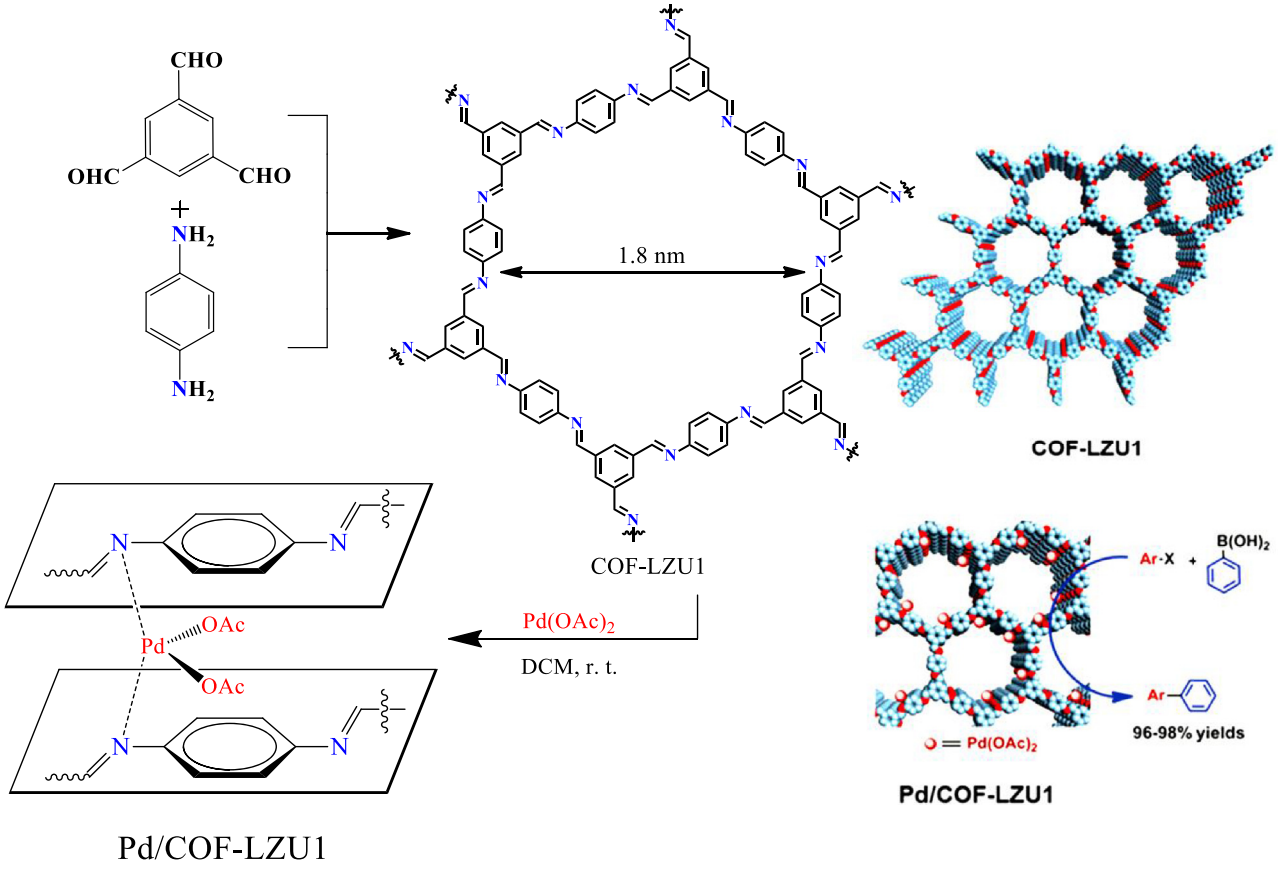

Fig. 15

Chemical and extended structures of COF-LZU1 and Pd/COF-LZU1. (Reproduced from Ref. [65] with permission; copyright 2011, American Chemical Society).

orientation of the polycrystalline DAAQ-TFP COF causing poor electrical contact (**Fig. 16(b)**). This problem was solved through the formation of an oriented thin film of β-ketoenamine–linked 2D COF, resulting in a 400% increase in the capacitance of the electrode (**Fig. 16(a)**) [176]. Recently, we reported supercapacitors incorporating various COFs featuring a diverse array of redox-active moieties (triaryltriazine, amino, pyridine, and carbazole units) and N-atom-rich groups (triazine, benzobisoxazole, and triphenylamine units) [30, 40, 77, 177,178]. These COFs exhibited good electrochemical properties because of their high surface areas, ordered porosities, and redox-active and N-atom-rich units.

5.4 Photovoltaics

COFs are an emerging versatile class of porous organic crystalline materials that could be used for solar energy conversion applications by the incorporation of organic chromophores as building blocks. Several methods have reported to construct electroactive COFs as active layers for bulk heterojunction solar cells, through the embedding of organic chromophores into the COF frameworks. These sites can generate singlet excitons under illumination, and act as electron D units in the presence of a suitable A unit chromophores embedded in the COF pores. Another strategy involves providing electron D moieties at adjacent linkers in the same monolayer [179].

5.4.1 COFs as electroactive materials

The ability of transport charge along the frameworks of COFs was firstly investigated by Jiang et al., through the construction of two semiconductive and photoconductive COFs, TP-COF (**Fig. 20a**) [180] and PPy-COF [35], based on a highly ordered π-conjugated pyrene derivative. TP-COF displayed the semiconducting characteristics and the strong blue light emission. TP-COF had the ability to harvest photons over a broad range of wavelengths—from the UV to the visible region—and also convert them to the blue emission. This emission arose after intramolecular singlet energy transfer from triphenylene to pyrene groups, suggesting electronic coupling of building blocks in COF structures. Moreover, TP-COF generated a current of 4.3 nA, which increased significantly to 20 nA after doping with I_2, suggesting p-type semiconducting characteristics (**Figs. 20b and 20c**). In addition, PPy-COF (**Fig. 20b**) could harvest visible light and generate a photocurrent of 5 nA with a Xenon lamp upon illumination.

5.4.2 2D COFs based on π-electron-rich macrocycles

To enhance the charge transport and visible photon harvesting capability, incorporating π-electron-rich macrocycles, such as porphyrin and phthalocyanine, into COF frameworks can broaden their optical absorption profiles. Porphyrin and phthalocyanine are two large π-systems having 18 π-electrons,

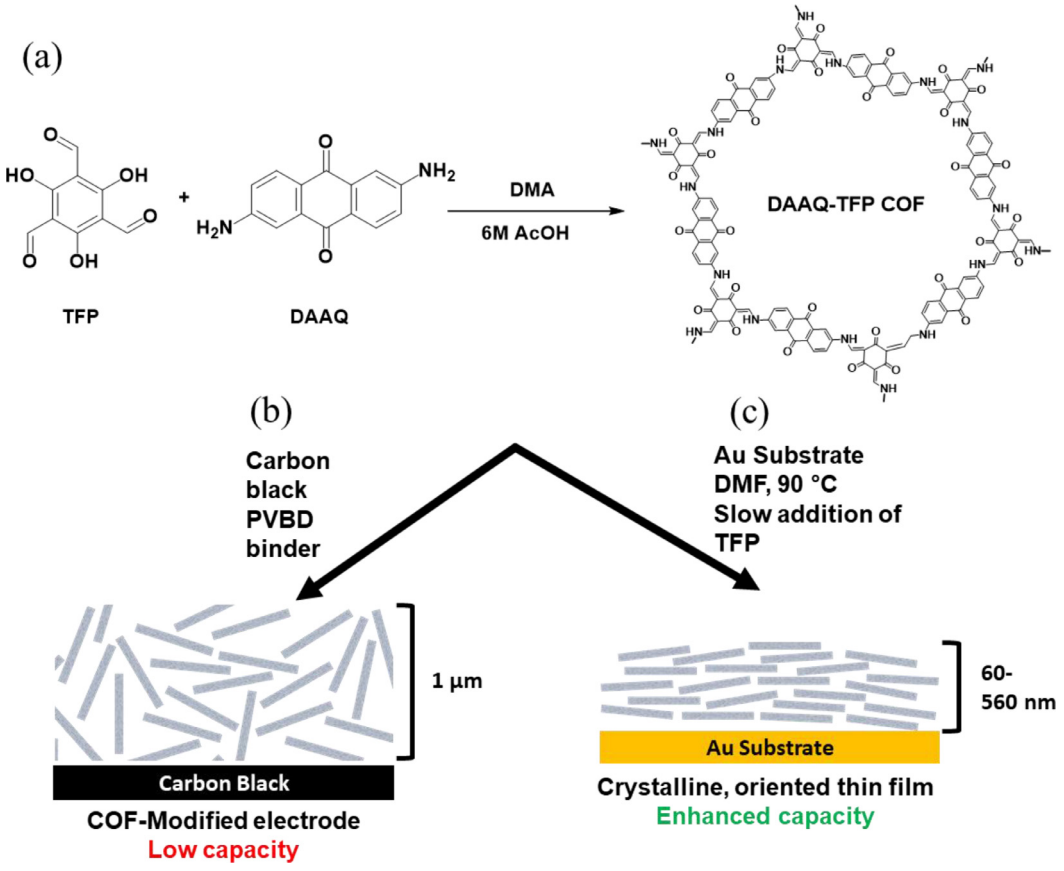

Fig. 16

(a) Schematic representation for synthesis of DAAQ-TFP. (b) COF electrode prepared from a slurry of DAAQ-TFP mixed with carbon black and a poly(vinylidene fluoride) binder. (c) Oriented thin film of DAAQ-TFP on Au electrodes.

in the form of planar continuous cycles, that have the ability to incorporate central metal ions. Jiang and co-workers studied the charge carrier transport properties of three different 2D porphyrin-based COFs incorporating various central metals (MP-COFs; $M = H_2$, Zn, Cu; **Fig. 17**) [181]. Flash-photolysis time-resolved microwave conductivity revealed that the resultant COFs had various types of charge mobilities, with the metal-free porphyrin H_2P-COF having hole transporting ability and the CuP-COF exhibiting electron transport capability. Interestingly, ZnP-COF displayed ambipolar charge transport ability. In these cases, the metal ions in the porphyrins played vital roles in both electron conduction (through the formation of metal-on-metal channels) and in tuning the carrier mobility. For example, the strong tendency of Cu metal to undergo ligand-to-metal charge transfer decreases of the porphyrin macrocycles electron density. As a result, CuP-COF facilitated electron transport by the metal-on-metal channel. In contrast, Zn metal did not undergo the ligand-to-metal charge transfer and favored balanced transport by both channels, leading to ambipolar conduction (**Fig. 17(b)**). Furthermore, it has been reported that hydrogen bonding in the porphyrin COF enhances the absorbance in the visible and near-infrared (NIR) regions and decreases the band gap [182].

The incorporation of metal phthalocyanine into COF frameworks has also been investigated. The high charge carrier mobilities of the well-ordered stacking layers in the π-systems of 2D metal phthalocyanine COFs led to high photoconductivity and panchromatic light response. For example, Jiang et al. introduced a well-ordered stacking unit (nickel phthalocyanine) into a COF structure. The resultant 2D NiPc-COF arranged into the layered structure of planar sheets with the uniform extended microporous channels, leading to light-harvesting capability in the visible and NIR regions and facilitated charge carrier transport (**Fig. 18**). Furthermore, the porous channels behaved as hosts for counterpart molecules that could fill the nano spaces, thereby further modulating the properties of the COFs [183]. The role of the central metal ion was investigated through the construction of three metallophthalocyanine COFs [184]. The central metal ions of the metal phthalocyanine groups strongly affected the charge carrier transport behavior and the absorption of light, in terms of both broadness and intensity.

5.4.3 Donor-Acceptor heterojunction systems

Another strategy for enhancing charge carrier transport and light absorption is the use of electron D/A systems, which feature electron-withdrawing A units alternately aligned with the D moieties. The D–A COF system using phthalocyanine (D) and benzothiadiazole (A) exhibited periodic d-on-D and A-on-A segregated channels, providing vertically oriented D and A heterojunction arrays, that supported the transport of holes and electrons by the aligned D and A columns.

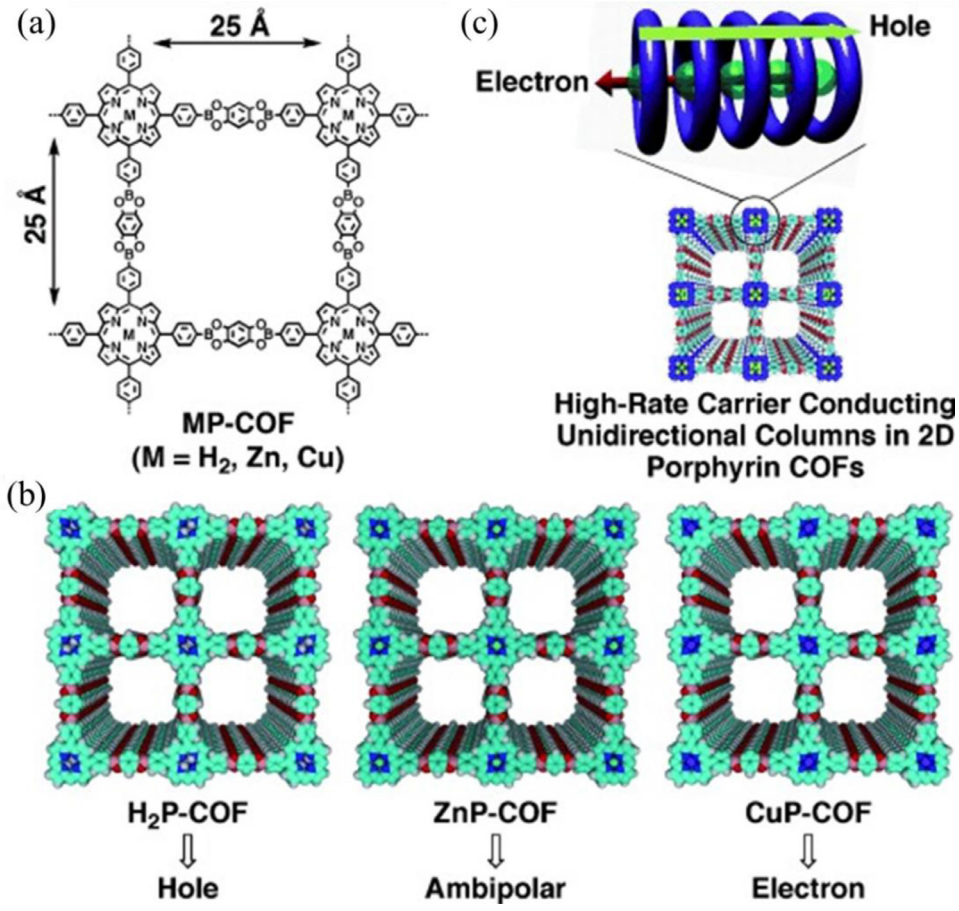

Fig. 17

(a, b) Schematic representations of (a) MP-COFs and (b) a 2 × 2 grid of MP-COFs with achiral AA stacking 2D sheets, and (c) Representation of the metal-on-metal and macrocycle-on-macrocycle channels for respective electron and hole transport in the stacked porphyrin columns of the 2D porphyrin COF. (Reproduced from Ref. [181] with permission; copyright 2015, American Chemical Society).

(**Fig. 19(a)**) Interestingly, carrier transport followed a different path than that of the n-type phthalocyanine COF; in the latter, the phthalocyanine columns were responsible for the carrier transport, while in the D–A system, the columns of benzothiadiazole formed the electron transport path [185].

In this context, another strategy to develop D–A COFs has been proposed by the filling spatially confining a units in the 1D open channels of electron-donating COFs. For example, Bein et al. developed a periodic interpenetrated structurally ordered D–A network using a thienothiophene-based COF (TT-COF) as the D units with open-pore channels of 3 nm; this open framework was capable of hosting fullerene derivative PCBM as a units through physical filling (**Fig. 19(b)**). Spectroscopic measurements revealed light-induced charge transfer from the photoconductive TT-COF network to the encapsulated fullerene A units in the pore structure [186]. The feasibility of photoinduced charge separation and collection within these systems make them great candidates for use in photovoltaic cells. Another method for exploiting the open channels of electron-donating COFs to construct D–A heterojunctions was realized through click reactions of channel walls with electron A moieties. For example, the click reactions of electron-donating COFs featuring different contents of N_3 groups on their channel walls have been performed with fullerene-derivative A units (**Fig. 19(c) and 19(d)**) [72]. A higher fullerene content led to stronger absorbance of visible light and higher-efficiency charge separation.

5.4.4 Fully π-conjugated systems

Recently, a fully π-conjugated system was synthesized from all-sp^2-hybridized carbon atoms extended in the 2D lattice with π-conjugation extended along both the *x*- and *y*-directions. The sp^2 c-COF displayed the oxidation potential at 0.94 V and the reduction potential at –0.96 V, giving the narrow band gap of 1.90 eV. Moreover, the conductivity of sp^2 c-COF was increased by 12 orders of magnitude after doping with I_2, reaching up to 7.1×10^{-2} S m^{-1}. By changing the linking group and forming an extended π-conjugation system, the optical colors of the resultant COFs could be changed: sp^2c-COF was red, the imine-linked 2D COF was yellow, and the model compound was yellow-orange [113].

5.4.5 Thin films covalent organic frameworks

Because thin films are highly preferable for practical applications in photoelectronic devices, the development of COF-

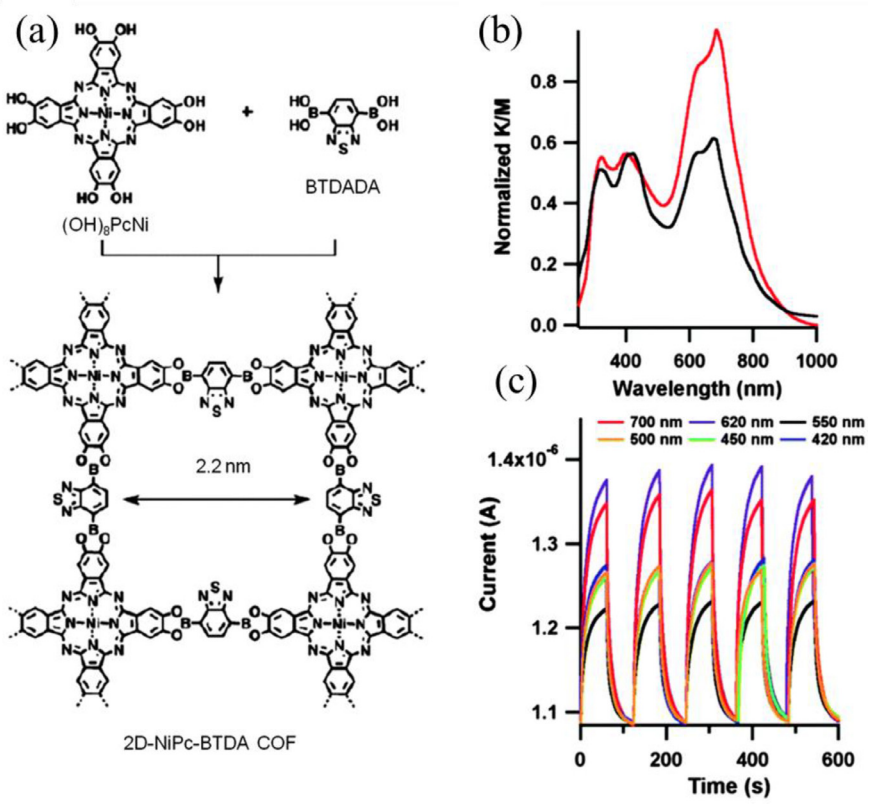

Fig. 18

(a) Representation of the synthesis of NiPc-BTDA. (b) Absorbance spectra of $(MeO)_8PcNi$ (black) and 2D-NiPc-BTDA COF (red). (c) Photocurrent of on–off switching of 2D-NiPc-BTDA COF under a bias voltage of 1.0 V at various wavelengths (Reproduced from Ref. [183] with permission; copyright 2015, Wiley).

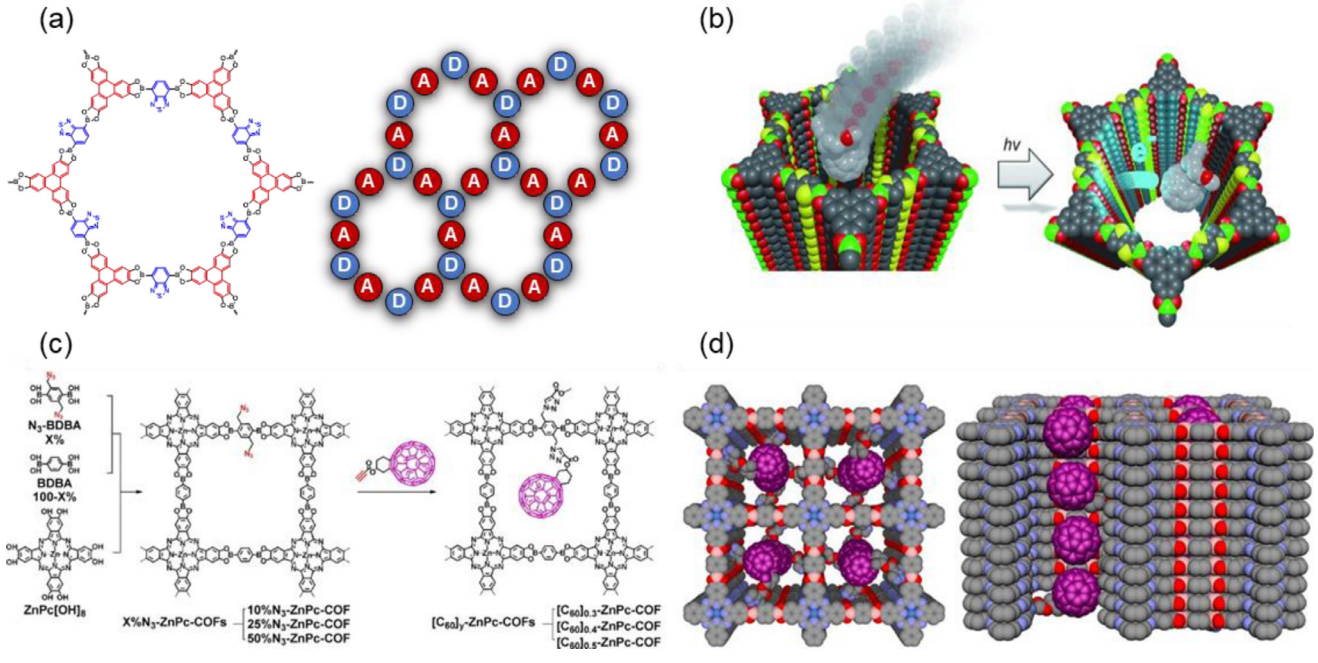

Fig. 19

(a) Representation of a 2D D–A COF featuring the self-sorted and periodic D–A ordering and bicontinuous conducting channels. (b) Illustration of the host–guest complex of COF channels loaded with fullerene units. (c, d) Schematic representation of the conversion of open lattice structures into segregated D–A arrays (Reproduced from Ref. [72] with permission; copyright 2014 American Chemical Society).

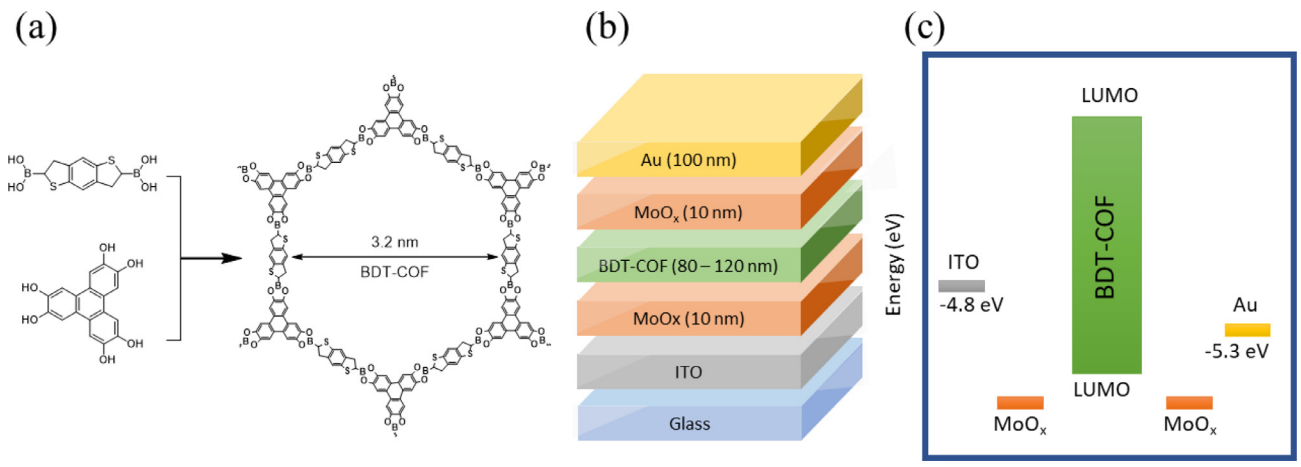

Fig. 20

(a) Schematic representation of the BDT-COF structure. (b) Architecture of the COF hole-only device. (c) Corresponding energy diagram of the system.

based thin films has been investigated, along with measurements of their electronic behavior [138,187]. Dichtel et al. exploited the high orientation and crystallinity of COF thin film on the SLG/SiO_2 substrate to prepare the photovoltaic device featuring designed functional π-electron system. These crystalline and aligned triphenylene–pyrene COF and phthalocyanine COF thin films on SLG/SiO_2 surfaces were used for further applications [137]. Moreover, TTF building blocks have been used as the electroactive units to construct the semiconducting COFs [188]. Since the charge-carrier mobility was high in those bulk COFs; however, the insoluble powder nature of the COFs limited their applications. To tackle this problem, Liu et al. constructed the oriented TTF-COF thin film and studied their doping-related conductivities [189]. The porous structure of the TTF-COF thin film enabled the incorporation of electron acceptor, including I_2 and tetracyanoquinodimethane (TCNQ), as charge-transfer partners. Liu et al. fabricated thin TTF-COF films and used the Au/Cr electrode to detect the relative conductivities. Compared with I–V curves before and after exposure to I_2 of the TTF-COF thin-film device revealed that the electronic conductivity increased by three orders of magnitude after doping.

Because electronic transport properties are influenced significantly by the molecular arrangement and film morphology [190], Bein et al. used an oriented BDT-COF thin-film device as the model system to investigate the directed charge carrier transport and the additional electrical property [191]. The degree of charge-carrier transport along the columnar stacks of COF thin film was an important factor determining the overall performance of the devices. Therefore, Bein et al. grew an oriented BDT-COF thin film on the ITO electrode coated with glass and employed MoO_x and Au as top electrodes (**Fig. 20**). By investigating the BDT-COF thin film performance at various thicknesses in the range 80–200 nm, they observed that the thinner COF film led to lower degrees of electronic defects and, hence, higher hole mobilities.

5.4.6 3D COFs as new platforms for next-generation photovoltaic devices

Recently, 3D COFs were employed as new platforms for next-generation crystalline organic photovoltaic devices [192]. Lopez and co-workers proposed the subphthalocyanine-based 3D COF capable of forming co-crystals with fullerene (C_{60}) through periodic ball-and-socket binding motifs [193]. The charge transport in this COF occurred through a charge-hopping mechanism between C_{60} units. Doping of the 3D COFs on perovskite solar cells (PSCs) increased the power efficiency and charge transport ability. For example, the simple bulk doping of 3D spirobifluorene-based COFs (SP-3D-COFs) on the PSCs enhanced the average power conversion efficiency substantially, by 15.9% for SP-3D-COF 1 and by 18.0% for SP-3D-COF 2, relative to that of the reference undoped PSC, while also decreasing the dark current and offering excellent leakage-prevention (**Fig. 21**) [68]. Moreover, the 3D dia framework of SP-3D-COFs provided numerous electron-transport channels in highly ordered alignment frameworks. To improve the charge transport in planar-type PSCs, a few layers of covalent organic nanosheets (CONs) exfoliated from COFs were employed as hole-transport layers together with poly(ethylenedioxythiophene):polystyrenesulfonate (PEDOT:PSS) [194]. The formed layers were used as an interlayer material in inverted planar PSCs. The power conversion efficiency (PCE) increased by 1% relative to that of the reference device, reaching a value of 10.2%. Furthermore, Zhong et al. used density functional theory to predict the properties of a quinazoline-based COF (Q-COF) exfoliated monolayer [195]. Their calculations suggested that the Q-COF would possess the direct band gap of 1.18 eV and the high absorption coefficient (10^5 cm^{-1}) in the visible and NIR regions (from 400 to 1000 nm). Furthermore, they observed that Q-COF and ZnSe monolayers had the ability to provide the heterojunction with a type-II band alignment, providing the photoelectric conversion efficiency of 16.89%, which could be further tuned to reach a value of 22.32%. These promising results

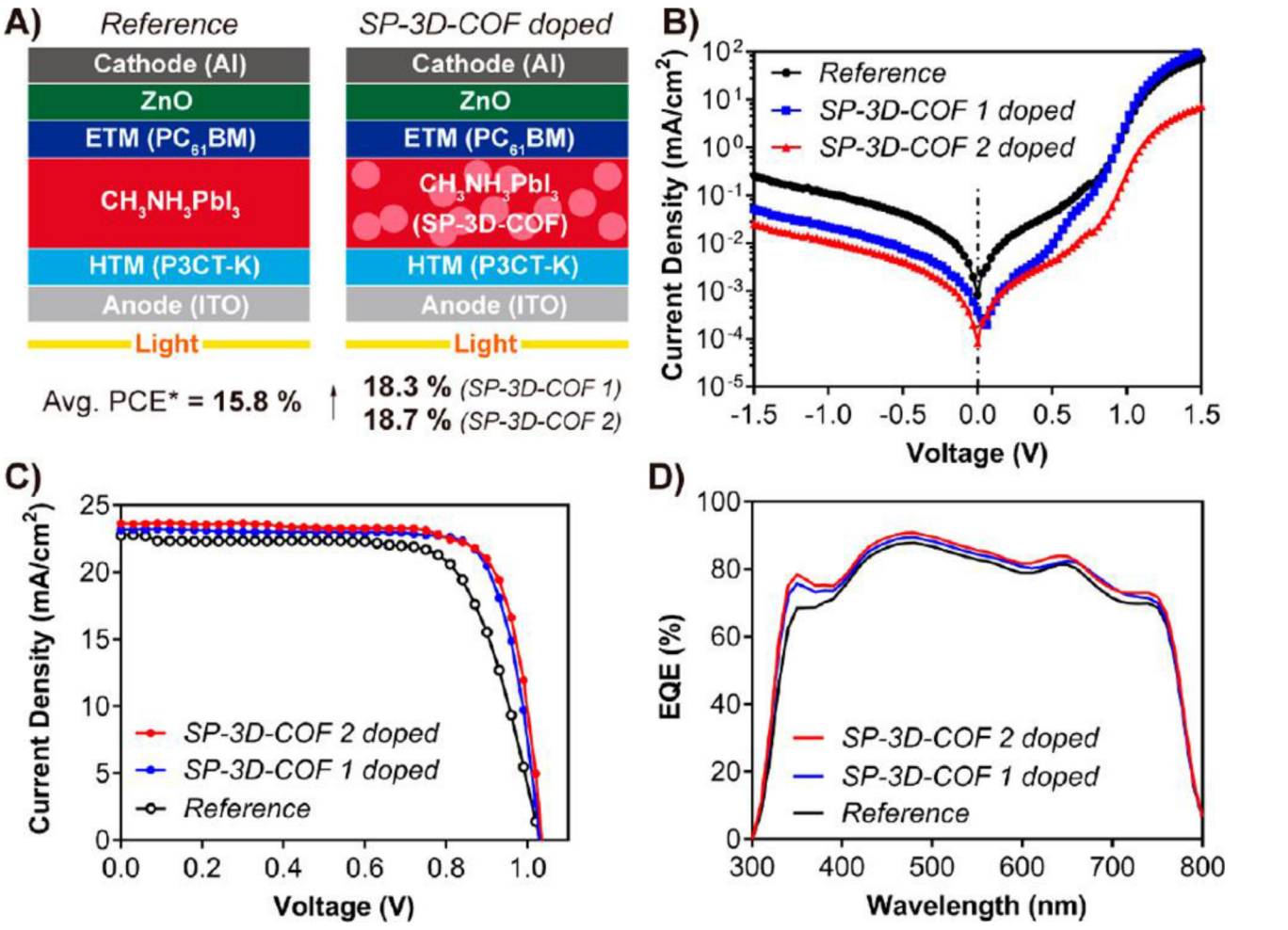

Fig. 21

(a) Device layout, (b) corresponding dark-currents density–voltage (*J–V*) curves, (c) *J–V* characteristic curves under AM 1.5 G 100 mW cm^{-2} simulated solar light, and (d) external quantum efficiency spectra of undoped reference and SP-3D-COF–doped PSC devices. (Reproduced from Ref. [68] with permission; copyright 2018 American Chemical Society).

should motivate further explorations of Q-COF monolayers as excellent 2D photovoltaic materials in optoelectronic devices, especially in solar cells.

Future perspectives and conclusions

COFs have been studied extensively as an attractive class of crystalline porous polymers. The superiority of COFs over other porous materials (*e.g.*, inorganic zeolites and MOFs) is undeniable—in terms of their predictable design and structural diversity. COFs have proven to be useful platforms for many applications, thanks to their low densities, high specific surface areas, and adjustable properties and functions. They have practical utility in a wide range of fields, including gas storage and separation, heterogeneous catalysis, chemical sensing, luminescence, electronic devices, drug delivery, and energy storage and conversion. In this Review, we discuss many of the advances that have occurred in COF research: the design principles and structural diversity of COFs (including the linking types), the synthetic techniques that have been developed for their preparation (with relevant examples), and some applications in which they have displayed excellent performance—namely CO_2 uptake, catalysis, supercapacitors, and photovoltaics. Although many challenges remain, the rapid advancement of COFs in the past few years heralds a promising future for these materials. As mentioned in Fig. 1(A), several topologies of COFs have been constructed through mediated the building units and compared with other porous materials, the resulting COF topology could be determined experimentally and theoretically by the dimensions and geometry of building blocks. The new COF materials connected the Archimedean tiling patterns such as [3^6, 4^4, 6^3, 3,6,3,6] and [3^2,4,3,4] or even Frank-Kasper phases are also the next challenge topics [196-200]. The door is open wide for further exploration of the beneficial properties of these interesting materials.

Declaration of Competing Interest

The authors declared that they have no conflicts of interest to this work.

Acknowledgments

This study was supported financially by Ministry of Science and Technology, Taiwan, under contracts MOST 106-2221-E-110-067-MY3, 108-2638-E-002-003-MY2, 108-2218-E-110-013-MY3, and 108-2221-E-110-014-MY3.

References

[1] I. Nath, J. Chakraborty, F. Verpoort, Metal organic frameworks mimicking natural enzymes: a structural and functional analogy, Chem. Soc. Rev. 45 (2016) 4127–4170.

[2] L. Zhou, X. Luo, J. Gao, G. Liu, L. Ma, Y. He, Z. Huang, Y. Jiang, Facile synthesis of covalent organic framework derived Fe-COFs composites as a peroxidase-mimicking artificial enzyme, Nanoscale Adv. (2) (2020) 1036–1039.

[3] C. Zhang, D.A. Mcadams II, J.C. Grunlan, Nano/micro-manufacturing of bioinspired materials: a review of methods to mimic natural structures, Adv. Mater. 28 (2016) 6292–6321.

[4] Y.V. Kaneti, S. Dutta, M.S.A. Hossain, M.J.A. Shiddiky, K.L. Tung, F.K. Shieh, C.K. Tsung, K.C.W. Wu, Y. Yamauchi, Strategies for improving the functionality of zeolitic imidazolate frameworks: tailoring nanoarchitectures for functional applications, Adv. Mater. 29 (2017) 1700213.

[5] L. Yu, X. Shang, H. Chen, L. Xiao, Y. Zhu, J. Fan, A tightly-bonded and flexible mesoporous zeolite-cotton hybrid hemostat, Nature Commun 10 (2019) 1932.

[6] M. Manzano, M. Vallet-Regi, Mesoporous silica nanoparticles for drug delivery, Adv. Funct. Mater. 30 (2020) 1902634.

[7] W.C. Chen, M.M.M. Ahmed, C.F. Wang, C.F. Huang S. W. Kuo, Highly thermally stable mesoporous Poly (cyanate ester) featuring double-decker–shaped polyhedral silsesquioxane framework, Polymer (Guildf) 185 (2019) 121940.

[8] A.F.M. EL-Mahdy, T.C. Yu, S.W. Kuo, Synthesis of multiple heteroatom–doped mesoporous carbon/silica composites for supercapacitors, Chem. Eng. J. 414 (2021) 128796.

[9] A.F.M. EL-Mahdy, T.E. Liu, S.W. Kuo, Direct synthesis of nitrogen-doped mesoporous carbons from triazine-functionalized resol for CO_2 uptake and highly efficient removal of dyes, J. Hazard. Mater. 391 (2020) 122163.

[10] W.C. Chu, B.P. Bastakoti, Y.V. Kaneti, J.G. Li, H.R. Alamri, Z.A. Alothman, Y. Yamauchi, S.W. Kuo, Tailored design of bicontinuous gyroid mesoporous carbon and nitrogen-doped carbon from poly(ethylene oxide-b-caprolactone) diblock copolymers, Chem. Eur. J. 23 (2017) 13734–13741.

[11] J.G. Li, Y.F. Ho, M.M.M. Ahmed, H.C. Liang, S.W. Kuo, Mesoporous carbons templated by PEO-PCL block copolymers as electrode materials for supercapacitors, Chem. Eur. J. 25 (2019) 10456–10463.

[12] K.S. Lakhi, D.H. Park, K. Al-Bahily, W. Cha, B. Viswanathan, J.H. Choy, A. Vinu, Mesoporous carbon nitrides: synthesis, functionalization, and applications, Chem. Soc. Rev. 46 (2017) 72–101.

[13] A.F.M. EL-Mahdy, T.C. Yu, M.G. Mohamed, Shiao-Wei Kuo, Secondary structures of polypeptide-based diblock copolymers influence the microphase separation of templates for the fabrication of microporous carbons, Macromolecules 54 (2021) 1030–1042.

[14] B. Hatton, K. Landskron, W. Whitnall, D. Perovic, G.A. Ozin, Past, present, and future of periodic mesoporous organosilicas–The PMOs, Acc. Chem. Res. 38 (2005) 305–312.

[15] N. Mizoshita, T. Tani, S. Inagaki, Syntheses, properties and applications of periodic mesoporous organosilicas prepared from bridged organosilane precursors, Chem. Soc. Rev. 40 (2011) 789–800.

[16] A.I. Copper, Conjugated microporous polymers, Adv. Mater. 26 (2009) 1291–1295.

[17] Y. Xu, S. Jin, H. Xu, A. Nagai, D. Jiang, Conjugated microporous polymers: design, synthesis and application, Chem. Soc. Rev. 42 (2013) 8012–8031.

[18] M.G. Mohamed, N.Y. Liu, A.F.M. EL-Mahdy, S.W. Kuo, Ultrastable luminescent hybrid microporous polymers based on polyhedral oligomeric silsesquioxane for CO_2 uptake and metal ion sensing, Micropor. Mesopor. Mater. 311 (2021) 110695.

[19] A.M. Elewa, M.H. Elsayed, A.F.M. EL-Mahdy, C.L. Chang, L.Y. Ting, W.C. Lin, C.Y. Lu, H.H. Chou, Appl. Catal. B-Environ. 285 (2021) 119802.

[20] J.R. Long, O.M. Yaghi, The pervasive chemistry of metal–organic frameworks, Chem. Soc. Rev. 38 (2009) 1213–1214.

[21] A.G. Slater, A.I. Cooper, Porous materials. Function-led design of new porous materials, Science 348 (2015) 8075.

[22] M.S. Lohse, T. Bein, Covalent organic frameworks: structures, synthesis, and applications, Adv. Funct. Mater. 28 (2018) 1705553.

[23] A.P. Côté, A.I. Benin, N.W. Ockwig, M. O'Keeffe, A.J. Matzger, O.M. Yaghi, Chemistry: porous, crystalline, covalent organic frameworks, Science 310 (2005) 1166–1170.

[24] C.S. Diercks, O.M. Yaghi, The atom, the molecule, and the covalent organic framework, Science 355 (2017) 1585.

[25] H.M. El-Kaderi, J.R. Hunt, J.L. Mendoza-Cortés, A.P. Côté, R.E. Taylor, M. O'Keeffe, O.M. Yaghi, Designed synthesis of 3D covalent organic frameworks, Science 316 (2007) 268–272.

[26] S.Y. Ding, W. Wang, Covalent organic frameworks (COFs): from design to applications, Chem. Soc. Rev. 42 (2013) 548–568.

[27] R.K. Sharma, P. Yadav, M. Yadav, R. Gupta, P. Rana, A. Srivastava, R. Zbořil, R.S. Varma, M. Antonietti, M.B. Gawande, Recent development of covalent organic frameworks (COFs): synthesis and catalytic (organic-electro-photo) applications, Mater. Horizons 7 (2020) 411–454.

[28] N. Huang, P. Wang, D. Jiang, Covalent organic frameworks: a materials platform for structural and functional designs, Nat. Rev. Mater. 1 (2016) 1–19.

[29] X. Chen, N. Huang, J. Gao, H. Xu, F. Xu, D. Jiang, Towards covalent organic frameworks with predesignable and aligned open docking sites, Chem. Commun. 50 (2014) 6161–6163.

[30] A.F.M. El-Mahdy, Y.H. Hung, T.H. Mansoure, H.H. Yu, T. Chen, S.W. Kuo, A hollow microtubular triazine-and benzobisoxazole-based covalent organic framework presenting sponge-like shells that functions as a high-performance supercapacitor, Chem. Asian J. 14 (2019) 1429–1435.

[31] X. Guan, F. Chen, Q. Fang, S. Qiu, Design and applications of three dimensional covalent organic frameworks, Chem. Soc. Rev. 49 (2020) 1357–1384.

[32] K. Geng, T. He, R. Liu, S. Dalapati, K.T. Tan, Z. Li, S. Tao, Y. Gong, Q. Jiang, D. Jiang, Covalent organic frameworks: design, synthesis, and functions, Chem. Rev. 120 (2020) 8814–8933.

[33] S. Kandambeth, A. Mallick, B. Lukose, M.V. Mane, T. Heine, R. Banerjee, Construction of crystalline 2D covalent organic frameworks with remarkable chemical (Acid/Base) stability via a combined reversible and irreversible route, J. Am. Chem. Soc. 134 (2012) 19524–19527.

[34] Z.J. Li, S.Y. Ding, H.D. Xue, W. Cao, W. Wang, Synthesis of -CN- linked covalent organic frameworks: via the direct condensation of acetals and amines, Chem. Commun. 52 (2016) 7217–7220.

[35] S. Wan, J. Guo, J. Kim, H. Ihee, D. Jiang, A photoconductive covalent organic framework: self-condensed arene cubes composed of eclipsed 2D polypyrene sheets for photocurrent generation, Angew. Chem. Int. Ed. 48 (2009) 5439–5442.

[36] K.T. Jackson, T.E. Reich, H.M. El-Kaderi, Targeted synthesis of a porous borazine-linked covalent organic framework, Chem. Commun. 48 (2012) 8823–8825.

[37] A.P. Côté, H.M. El-Kaderi, H. Furukawa, J.R. Hunt, O.M. Yaghi, Reticular synthesis of microporous and mesoporous 2D covalent organic frameworks, J. Am. Chem. Soc. 129 (2007) 12914–12915.

[38] Y.F. Xie, S.Y. Ding, J.M. Liu, W. Wang, Q.Y. Zheng, Triazatruxene based covalent organic framework and its quick-response fluorescence-on nature towards electron rich arenes, J. Mater. Chem. C 3 (2015) 10066–10069.

[39] L. Xu, S.Y. Ding, J. Liu, J. Sun, W. Wang, Q.Y. Zheng, Highly crystalline covalent organic frameworks from flexible building blocks, Chem. Commun. 52 (2016) 4706–4709.

[40] A.F.M. El-Mahdy, C.H. Kuo, A. Alshehri, C. Young, Y. Yamauchi, J. Kim, S.W. Kuo, Strategic design of triphenylamine- and triphenyltriazine-based two-dimensional covalent organic frameworks for CO2 uptake and energy storage, J. Mater. Chem. A 6 (2018) 19532–19541.

[41] A.F.M. EL-Mahdy, C. Young, J. Kim, J. You, Y. Yamauchi, S.W. Kuo, Hollow microspherical and microtubular [3+3] carbazole-based covalent organic frameworks and their gas and energy storage applications, ACS Appl. Mater. Interfaces 11 (2019) 9343–9354.

[42] H.R. Abuzeid, A.F.M. El-Mahdy, M.M.M. Ahmed, S.W. Kuo, Triazine-functionalized covalent benzoxazine framework for direct synthesis of N-doped microporous carbon, Polym. Chem. 10 (2019) 6010–6020.

[43] X. Chen, J. Gao, D. Jiang, Designed synthesis of porphyrin-based two-dimensional covalent organic frameworks with highly ordered structures, Chem. Lett. 44 (2015) 1257–1259.

[44] E.L. Spitler, W.R. Dichtel, Lewis acid-catalysed formation of two-dimensional phthalocyanine covalent organic frameworks, Nat. Chem. 2 (2010) 672–677.

[45] S. Dalapati, S. Jin, J. Gao, Y. Xu, A. Nagai, D. Jiang, An azine-linked covalent organic framework, J. Am. Chem. Soc. 135 (2013) 17310–17313.

[46] T.Y. Zhou, S.Q. Xu, Q. Wen, Z.F. Pang, X. Zhao, One-step construction of two different kinds of pores in a 2D covalent organic framework, J. Am. Chem. Soc. 136 (2014) 15885–15888.

[47] Z.F. Pang, T.Y. Zhou, R.R. Liang, Q.Y. Qi, X. Zhao, Regulating the topology of 2D covalent organic frameworks by the rational introduction of substituents, Chem. Sci. 8 (2017) 3866–3870.

[48] H.R. Abuzeid, A.F.M. EL-Mahdy, S.W. Kuo, Hydrogen bonding induces dual porous types with microporous and mesoporous covalent organic frameworks based on bicarbazole units, Microporous Mesoporous Mater 300 (2020) 110151.

[49] S. Dalapati, M. Addicoat, S. Jin, T. Sakurai, J. Gao, H. Xu, S. Irle, S. Seki, D. Jiang, D. Rational design of crystalline supermicroporous covalent organic frameworks with triangular topologies, Nat. Commun. 6 (2015) 1–8.

[50] Z.F. Pang, S.Q. Xu, T.Y. Zhou, R.R. Liang, T.G. Zhan, X. Zhao, Construction of covalent organic frameworks bearing three different kinds of pores through the heterostructural mixed linker strategy, J. Am. Chem. Soc. 138 (2016) 4710–4713.

[51] X. Kang, X. Han, C. Yuan, C. Cheng, Y. Liu, Y. Cui, Reticular synthesis of tbo topology covalent organic frameworks, J. Am. Chem. Soc. 142 (2020) 16346–16356.

[52] H. Li, J. Ding, X. Guan, F. Chen, C. Li, L. Zhu, M. Xue, D. Yuan, V. Valtchev, Y. Yan, S. Qiu, Three-dimensional large-pore covalent organic framework with stp topology, J. Am. Chem. Soc. 142 (2020) 13334–13338.

[53] N. Huang, L. Zhai, D.E. Coupry, M.A. Addicoat, K. Okushita, K. Nishimura, T. Heine, D. Jiang, Multiple-component covalent organic frameworks, Nat. commun. 7 (2016) 1–12.

[54] Y. Tian, S.Q. Xu, C. Qian, Z.F. Pang, G.F. Jiang, X. Zhao, Two-dimensional dual-pore covalent organic frameworks obtained from the combination of two D 2h symmetrical building blocks, Chem. Commun. 52 (2016) 11704–11707.

[55] F.J. Uribe-Romo, J.R. Hunt, H. Furukawa, C. Klöck, M. O'Keeffe, O.M. Yaghi, A crystalline imine-linked 3-D porous covalent organic framework, J. Am. Chem. Soc. 131 (2009) 4570–4571.

[56] Q. Fang, J. Wang, S. Gu, R.B. Kaspar, Z. Zhuang, J. Zheng, H. Guo, S. Qiu, Y. Yan, 3D porous crystalline polyimide covalent organic frameworks for drug delivery, J. Am. Chem. Soc. 137 (2015) 8352–8355.

[57] C. Wu, Y. Liu, H. Liu, C. Duan, Q. Pan, J. Zhu, F. Hu, X. Ma, T. Jiu, Z. Li, Y. Zhao, Highly conjugated three-dimensional covalent organic frameworks based on spirobifluorene for perovskite solar cell enhancement, J. Am. Chem. Soc. 140 (2018) 10016–10024.

[58] X. Han, J. Huang, C. Yuan, Y. Liu, Y. Cui, Chiral 3D covalent organic frameworks for high performance liquid chromatographic enantioseparation, J. Am. Chem. Soc. 140 (2018) 892–895.

[59] S. Yan, X. Guan, H. Li, D. Li, M. Xue, Y. Yan, V. Valtchev, S. Qiu, Q. Fang, Three-dimensional Salphen-based covalent–organic frameworks as catalytic antioxidants, J. Am. Chem. Soc. 141 (2019) 2920–2924.

[60] G. Lin, H. Ding, D. Yuan, B. Wang, C. Wang, A pyrene-based, fluorescent three-dimensional covalent organic framework, J. Am. Chem. Soc. 138 (2016) 3302–3305.

[61] G. Lin, H. Ding, R. Chen, Z. Peng, B. Wang, C. Wang, 3D porphyrin-based covalent organic frameworks, J. Am. Chem. Soc. 139 (2017) 8705–8709.

[62] C. Gao, J. Li, S. Yin, G. Lin, T. Ma, Y. Meng, J. Sun, C. Wang, Isostructural three-dimensional covalent organic frameworks, Angew. Chem., Int. Ed. 58 (2019) 9770–9775.

[63] H.M. El-Kaderi, J.R. Hunt, J.L. Mendoza-Cortés, A.P. Côté, R.E. Taylor, M. O'Keeffe, O.M. Yaghi, Designed synthesis of 3D covalent organic frameworks, Science 316 (2007) 268–272.

[64] D. Cao, J. Lan, W. Wang, B. Smit, Lithium-doped 3D covalent organic frameworks: high-capacity hydrogen storage materials, Angew. Chem., Int. Ed. 48 (2009) 4824–4827.

[65] D.N. Bunck, W.R. Dichtel, Internal functionalization of three-dimensional covalent organic frameworks, Angew. Chem., Int. Ed. 51 (2012) 1885–1889.

[66] D.N. Bunck, W.R. Dichtel, Postsynthetic functionalization of 3D covalent organic frameworks, Chem. Commun. 49 (2013) 2457–2459.

[67] L.A. Baldwin, J.W. Crowe, D.A. Pyles, P.L. McGrier, Metalation of a mesoporous three-dimensional covalent organic framework, J. Am. Chem. Soc. 138 (2016) 15134–15137.

[68] C. Wu, Y. Liu, H. Liu, C. Duan, Q. Pan, J. Zhu, F. Hu, X. Ma, T. Jiu, Z. Li, Y. Zhao, Highly conjugated three-dimensional covalent organic frameworks based on spirobifluorene for perovskite solar cell enhancement, J. Am. Chem. Soc. 140 (2018) 10016–10024.

[69] Y. Lan, X. Han, M. Tong, H. Huang, Q. Yang, D. Liu, X. Zhao, C. Zhong, Materials genomics methods for high-throughput construction of COFs and targeted synthesis, Nat. Commun. 9 (2018) 5274.

[70] Y. Liu, Y. Ma, Y. Zhao, X. Sun, F. Gándara, H. Furukawa, Z. Liu, H. Zhu, C. Zhu, K. Suenaga, P. Oleynikov, Weaving of organic threads into a crystalline covalent organic framework, Science 351 (2016) 365–369.

[71] E.L. Spitler, B.T. Koo, J.L. Novotney, J.W. Colson, F.J. Uribe-Romo, G.D. Gutierrez, P. Clancy, W.R. Dichtel, A 2D covalent organic framework with 4.7-nm pores and insight into its interlayer stacking, J. Am. Chem. Soc. 133 (2011) 19416–19421.

[72] L. Chen, K. Furukawa, J. Gao, A. Nagai, T. Nakamura, Y. Dong, D. Jiang, Photoelectric covalent organic frameworks: converting open lattices into ordered donor–acceptor heterojunctions, J. Am. Chem. Soc. 136 (2014) 9806–9809.

[73] S.Y. Ding, J. Gao, Q. Wang, Y. Zhang, W.G. Song, C.Y. Su, W. Wang, Construction of covalent organic framework for catalysis: pd/COF-LZU1 in Suzuki–Miyaura coupling reaction, J. Am. Chem. Soc. 133 (2011) 19816–19822.

[74] J.L. Segura, M.J. Mancheño, F. Zamora, Covalent organic frameworks based on Schiff-base chemistry: synthesis, properties and potential applications, Chem. Soc. Rev. 45 (2016) 5635–5671.

[75] D.M. Fischbach, G. Rhoades, C. Espy, F. Goldberg, B.J. Smith, Controlling the crystalline structure of imine-linked 3D covalent organic frameworks, Chem. Commun. 55 (2019) 3594–5397.

[76] X. Wu, B. Wang, Z. Yang, L. Chen, Novel imine-linked covalent organic frameworks: preparation, characterization and application, J. Mater. Chem. A. 7 (2019) 5650–5655.

[77] A.F.M. EL-Mahdy, M.B. Zakaria, H.X. Wang, T. Chen, Y. Yamauchi, S.W. Kuo, Heteroporous bifluorenylidene-based covalent organic frameworks displaying exceptional dye adsorption behavior and high energy storage, J. Mater. Chem. A 8 (2020) 25148–25155.

[78] M.G. Rabbani, A.K. Sekizkardes, Z. Kahveci, T.E. Reich, R. Ding, H.M. El-Kaderi, A 2D mesoporous imine-linked covalent organic framework for high pressure gas storage applications, Chem. Eur. J. 19 (2013) 3324–3328.

[79] Q. Gao, X. Li, G.H. Ning, K. Leng, B. Tian, C. Liu, W. Tang, H. Sen Xu, K.P. Loh, Highly photoluminescent two-dimensional imine-based covalent organic frameworks for chemical sensing, Chem. Commun. 54 (2018) 2349–2352.

[80] C. Montoro, D. Rodríguez-San-Miguel, E. Polo, R. Escudero-Cid, M.L. Ruiz-González, J.A.R. Navarro, P. Ocón, F. Zamora, Ionic conductivity and potential application for fuel cell of a modified imine-based covalent organic framework, J. Am. Chem. Soc. 139 (2017) 10079–10086.

[81] S.B. Alahakoon, C.M. Thompson, G. Occhialini, R.A. Smaldone, Design principles for covalent organic frameworks in energy storage applications, ChemSusChem 10 (2017) 2116–2129.

[82] A.F.M. EL-Mahdy, A.M. Elewa, S. Huang, H. Chou, S.W. Kuo, Dual-function fluorescent covalent organic frameworks: HCl sensing and photocatalytic H_2 evolution from water, Adv. Opt. Mater. 8 (2020) 2000641.

[83] A.F.M. EL-Mahdy, M.Y. Lai, S.W. Kuo, Highly fluorescent covalent organic framework as hydrogen chloride sensor: roles of Schiff base bonding and π-stacking, J. Mater. Chem. C. 8 (2020) 9520–9528.

[84] W.L. Dong, S.Y. Li, J.Y. Yue, C. Wang, D. Wang, L.J. Wan, Fabrication of bilayer tetrathiafulvalene integrated surface covalent organic frameworks, Phys. Chem. Chem. Phys. 18 (2016) 17356–17359.

[85] S. Dalapati, M. Addicoat, S. Jin, T. Sakurai, J. Gao, H. Xu, S. Irle, S. Seki, D. Jiang, Rational design of crystalline supermicroporous covalent organic frameworks with triangular topologies, Nat. Commun. 6 (2015) 7786.

[86] C. Krishnaraj, A.M. Kaczmarek, H.S. Jena, K. Leus, N. Chaoui, J. Schmidt, R.V. Deun, P.V.D. Voort, Triggering white-light emission in a 2D imine covalent organic framework through lanthanide augmentation, ACS Appl. Mater. Interfaces 11 (2019) 27343–27352.

[87] E.M. Johnson, R. Haiges, S.C. Marinescu, Covalent-organic frameworks composed of rhenium bipyridine and metal porphyrins: designing heterobimetallic frameworks with two distinct metal sites, ACS Appl. Mater. Interfaces 10 (2018) 37919–37927.

[88] D.A. Popov, J.M. Luna, N.M. Orchanian, R. Haiges, C.A. Downesa, S.C. Marinescu, A 2,2′-bipyridine-containing covalent organic framework bearing rhenium (i) tricarbonyl moieties for CO_2 reduction, Dalton Trans 47 (2018) 17450–17460.

[89] D. Li, C. Li, L. Zhang, H. Li, L. Zhu, D. Yang, Q. Fang, S. Qiu, X. Yao, Metal-free thiophene-sulfur covalent organic frameworks: precise and controllable synthesis of catalytic active sites for oxygen reduction, J. Am. Chem. Soc. 142 (2020) 8104–8108.

[90] F.J. Uribe-Romo, J.R. Hunt, H. Furukawa, C. Klöck, M. O'Keeffe, O.M. Yaghi, A crystalline imine-linked 3-D porous covalent organic framework, J. Am. Chem. Soc. 131 (2009) 4570–4571.

[91] Y.B. Zhang, J. Su, H. Furukawa, Y. Yun, F. Gándara, A. Duong, X. Zou, O.M. Yaghi, Single-crystal structure of a covalent organic framework, J. Am. Chem. Soc. 135 (2013) 16336–16339.

[92] Q. Fang, S. Gu, J. Zheng, Z. Zhuang, S. Qiu, Y. Yan, 3D microporous base-functionalized covalent organic frameworks for size-selective catalysis, Angew. Chem. Int. Ed. 53 (2014) 2922–2926.

[93] Y.X. Ma, Z.J. Li, L. Wei, S.Y. Ding, Y.B. Zhang, W. Wang, A dynamic three-dimensional covalent organic framework, J. Am. Chem. Soc. 139 (2017) 4995–4998.

[94] Y. Wang, Y. Liu, H. Li, X. Guan, M. Xue, Y. Yan, V. Valtchev, S. Qiu, Q. Fang, Three-dimensional mesoporous covalent organic frameworks through steric hindrance engineering, J. Am. Chem. Soc. 142 (2020) 3736–3741.

[95] Y. Zhang, X. Shen, X. Feng, H. Xia, Y. Mu, X. Liu, Chem. Commun. 52 (2016) 11088–11091.

[96] L. Stegbauer, K. Schwinghammer, B.V. Lotsch, A hydrazone-based covalent organic framework for photocatalytic hydrogen production, Chem. Sci. 5 (2014) 2789–2793.

[97] L. Stegbauer, M.W. Hahn, A. Jentys, G. Savasci, C. Ochsenfeld, J.A. Lercher, B.V. Lotsch, Tunable water and CO_2 sorption properties in isostructural azine-based covalent organic frameworks through polarity engineering, Chem. Mater. 27 (2015) 7874–7881.

[98] S.B. Alahakoon, G.T. McCandless, A.A.K. Karunathilake, C.M. Thompson, R.A. Smaldone, Enhanced structural organization in covalent organic frameworks through fluorination, Chem. Eur. J. 23 (2017) 4255–4259.

[99] S.B. Alahakoon, C.M. Thompson, A.X. Nguyen, G. Occhialini, G.T. McCandless, R.A. Smaldone, An azine-linked hexaphenylbenzene based covalent organic framework, Chem. Commun. 52 (2016) 2843–2845.

[100] J. Lu, F. Lin, Q. Wen, Q.Y. Qi, J.Q. Xu, X. Zhao, Large-scale synthesis of azine-linked covalent organic frameworks in water and promoted by water, New J. Chem. 43 (2019) 6116–6120.

[101] X. Li, Y. Qi, G. Yue, Q. Wu, Y. Li, M. Zhang, X. Guo, X. Li, L. Ma, S. Li, Solvent-and catalyst-free synthesis of an azine-linked covalent organic framework and the induced tautomerization in the adsorption of U(VI) and Hg (II), Green Chem 21 (2019) 649–657.

[102] P. Guan, J. Qiu, Y. Zhao, H. Wang, Z. Li, Y. Shi, J. Wang, A novel crystalline azine-linked three-dimensional covalent organic framework for CO_2 capture and conversion, Chem. Commun. 55 (2019) 12459–12462.

[103] Q. Fang, Z. Zhuang, S. Gu, R.B. Kaspar, J. Zheng, J. Wang, S. Qiu, Y. Yan, Designed synthesis of large-pore crystalline polyimide covalent organic frameworks, Nat. Commun. 5 (2014) 4503.

[104] Q. Fang, J. Wang, S. Gu, R.B. Kaspar, Z. Zhuang, J. Zheng, H. Guo, S. Qiu, Y. Yan, 3D porous crystalline polyimide covalent organic frameworks for drug delivery, J. Am. Chem. Soc. 137 (2015) 8352–8355.

[105] H.L. Nguyen, C. Gropp, O.M. Yaghi, Reticulating 1D ribbons into 2D covalent organic frameworks by imine and imide linkages, J. Am. Chem. Soc. 142 (2020) 2771–2776.

[106] S. Wu, S. Gu, A. Zhang, G. Yu, Z. Wang, J. Jian, C. Pan, A rational construction of microporous imide-bridged covalent–organic polytriazines for high-enthalpy small gas absorption, J. Mater. Chem. A 3 (2015) 878–885.

[107] Y. Zhang, Z. Huang, B. Ruan, X. Zhang, T. Jiang, N. Ma, F.C. Tsai, Design and synthesis of polyimide covalent organic frameworks, Macromol. Rapid Commun. (2020), doi:10.1002/marc.202000402.

[108] S. Royuela, E. Martínez-Periñán, M.P. Arrieta, J.I. Martínez, M.M. Ramos, F. Zamora, E. Lorenzo, J.L. Segura, Oxygen reduction using a metal-free naphthalene diimide-based covalent organic framework electrocatalyst, Chem. Commun. 56 (2020) 1267–1270.

[109] A.F.M. EL-Mahdy, Y.H. Hung, T.H. Mansoure, H.H. Yu, Y.S. Hsu, K.C.W. Wu, S.W. Kuo, Synthesis of [3+3] β-ketoenamine-tethered covalent organic frameworks (COFs) for high-performance supercapacitance and CO_2 storage, J. Taiwan Inst. Chem. Eng. 103 (2019) 199–208.

[110] C.R. Deblase, K.E. Silberstein, T.T. Truong, H.D. Abruña, W.R. Dichtel, β-ketoenamine-linked covalent organic frameworks capable of pseudocapacitive energy storage, J. Am. Chem. Soc. 135 (2013) 16821–16824.

[111] L. Liu, W.K. Meng, Y.S. Zhou, X. Wang, G.J. Xu, M.L. Wang, J.M. Lin, R.S. Zhao, β-Ketoenamine-linked covalent organic framework coating for ultra-high-performance solid-phase microextraction of polybrominated diphenyl ethers from environmental samples, Chem. Eng. J. 356 (2019) 926–933.

[112] H. Wang, C. Qian, J. Liu, Y. Zeng, D. Wang, W. Zhou, L. Gu, H. Wu, G. Liu, Y. Zhao, Integrating suitable linkage of covalent organic frameworks into covalently bridged inorganic/organic hybrids toward efficient photocatalysis, J. Am. Chem. Soc. 142 (2020) 4862–4871.

[113] E. Jin, M. Asada, Q. Xu, S. Dalapati, M.A. Addicoat, M.A. Brady, H. Xu, T. Nakamura, T. Heine, Q. Chen, D. Jiang, Two-dimensional sp^2 carbon–conjugated covalent organic frameworks, Science 357 (2017) 673–676.

[114] E. Jin, J. Li, K. Geng, Q. Jiang, H. Xu, Q. Xu, D. Jiang, Designed synthesis of stable light-emitting two-dimensional sp2 carbon-conjugated covalent organic frameworks, Nat. Commun. 9 (2018) 4143.

[115] X. Zhuang, W. Zhao, F. Zhang, Y. Cao, F. Liu, S. Bi, X. Feng, A two-dimensional conjugated polymer framework with fully sp2-bonded carbon skeleton, Polym. Chem. 7 (2016) 4176–4181.

[116] R. Chen, J.L. Shi, Y. Ma, G. Lin, X. Lang, C. Wang, Designed synthesis of a 2D porphyrin-based sp^2 carbon-conjugated covalent organic framework for heterogeneous photocatalysis, Angew. Chem. Int. Ed. 58 (2019) 6430–6434.

[117] Y. Zhao, H. Liu, C. Wu, Z. Zhang, Q. Pan, F. Hu, R. Wang, P. Li, X. Huang, Z. Li, Fully conjugated two-dimensional sp^2-carbon covalent organic frameworks as artificial photosystem I with high efficiency, Angew. Chem. Int. Ed. 58 (2019) 5376–5381.

[118] H. Lyu, C.S. Diercks, C. Zhu, O.M. Yaghi, Porous crystalline olefin-linked covalent organic frameworks, J. Am. Chem. Soc. 141 (2019) 6848–6852.

[119] S. Bi, C. Yang, W. Zhang, J. Xu, L. Liu, D. Wu, X. Wang, Y. Han, Q. Liang, F. Zhang, Two-dimensional semiconducting covalent organic frameworks via condensation at arylmethyl carbon atoms, Nat. Commun. 10 (2019) 2467.

[120] J.R. Hunt, C.J. Doonan, J.D. LeVangie, A.P. Côté, O.M. Yaghi, Reticular synthesis of covalent organic borosilicate frameworks, J. Am. Chem. Soc. 130 (2008) 11872–11873.

[121] X. Guan, H. Li, Y. Ma, M. Xue, Q. Fang, Y. Yan, V. Valtchev, S. Qiu, Chemically stable polyarylether-based covalent organic frameworks, Nat. Chem. 11 (2019) 587–594.

[122] D. Zhou, X. Tan, H. Wu, L. Tian, M. Li, Synthesis of C– C bonded two-dimensional conjugated covalent organic framework films by Suzuki polymerization on a liquid–liquid interface, Angew. Chem. Int. Ed. 58 (2019) 1376–1381.

[123] H. Guo, M. Wang, R. Xue, J. Yao, X. Wang, L. Zhang, J. Liu, W. Yang, A new COF linked by an ether linkage (–O–): synthesis, characterization and application in supercapacitance, RSC Adv 9 (2019) 13458–13464.

[124] P. Kuhn, M. Antonietti, A. Thomas, Porous, covalent triazine-based frameworks prepared by ionothermal synthesis, Angew. Chem. Int. Ed. 47 (2008) 3450–3453.

[125] M. Liu, L. Guo, S. Jin, B. Tan, Covalent triazine frameworks: synthesis and applications, J. Mater. Chem. A. 7 (2019) 5153–5172.

[126] C. Gu, D. Liu, W. Huang, J. Liu, R. Yang, Synthesis of covalent triazine-based frameworks with high CO_2 adsorption and selectivity, Polym. Chem. 6 (2015) 7410–7417.

[127] P. Puthiaraj, Y.R. Lee, S. Zhang, W.S. Ahn, Triazine-based covalent organic polymers: design, synthesis and applications in heterogeneous catalysis, J. Mater. Chem. A. 4 (2016) 16288–16311.

[128] Y. Li, S. Zheng, X. Liu, P. Li, L. Sun, R. Yang, S. Wang, Z.S. Wu, X. Bao, W.Q. Deng, Conductive microporous covalent triazine-based framework for high-performance electrochemical capacitive energy storage, Angew. Chem. Int. Ed. 57 (2018) 7992–7996.

[129] L. Hao, S. Zhang, R. Liu, J. Ning, G. Zhang, L. Zhi, Bottom-up construction of triazine-based frameworks as metal-free electrocatalysts for oxygen reduction reaction, Adv. Mater. 27 (2015) 3190–3195.

[130] M.G. Mohamed, A.F.M. El-Mahdy, Y. Takashi, S.W. Kuo, Ultrastable conductive microporous covalent triazine frameworks based on pyrene moieties provide high-performance CO_2 uptake and supercapacitance, New J. Chem. 44 (2020) 8241–8253.

[131] X. Chen, M. Addicoat, E. Jin, H. Xu, T. Hayashi, F. Xu, N. Huang, S. Irle, D. Jiang, Designed synthesis of double-stage two-dimensional covalent organic frameworks, Sci. Rep. 5 (2015) 14650.

[132] Y. Zeng, R. Zou, Z. Luo, H. Zhang, X. Yao, X. Ma, R. Zou, Y. Zhao, Covalent organic frameworks formed with two types of covalent bonds based on orthogonal reactions, J. Am. Chem. Soc. 137 (2015) 1020–10123.

[133] H. Li, Q. Pan, Y. Ma, X. Guan, M. Xue, Q. Fang, Y. Yan, V. Valtchev, S. Qiu, Three-dimensional covalent organic frameworks with dual linkages for bifunctional cascade catalysis, J. Am. Chem. Soc. 138 (2016) 14783–14788.

[134] Y. Li, W. Chen, G. Xing, D. Jiang, L. Chen, New synthetic strategies toward covalent organic frameworks, Chem. Soc. Rev. 49 (2020) 2852–2868.

[135] M.E. Davis, Ordered porous materials for emerging applications, Nature 417 (2002) 813–821.

[136] H. Lu, C. Wang, J. Chen, R. Ge, W. Leng, B. Dong, J. Huang, Y. Gao, A novel 3D covalent organic framework membrane grown on a porous α-Al_2O_3 substrate under solvothermal conditions, Chem. Commun. 51 (2015) 15562–15565.

[137] J.W. Colson, A.R. Woll, A. Mukherjee, M.P. Levendorf, E.L. Spitler, V.B. Shields, M.G. Spencer, J. Park, W.R. Dichtel, Oriented 2D covalent organic framework thin films on single-layer graphene, Science 332 (2011) 228–231.

[138] H. Wang, Z. Zeng, P. Xu, L. Li, G. Zeng, R. Xiao, Z. Tang, D. Huang, L. Tang, C. Lai, D. Jiang, Y. Liu, H. Yi, L. Qin, S. Ye, X. Ren, W. Tang, Recent progress in covalent organic framework thin films: fabrications, applications and perspectives, Chem. Soc. Rev. 48 (2019) 488–516.

[139] M.J. Bojdys, J. Jeromenok, A. Thomas, M. Antonietti, Rational extension of the family of layered, covalent, triazine-based frameworks with regular porosity, Adv. Mater. 22 (2010) 2202–2205.

[140] X. Guan, Y. Ma, H. Li, Y. Yusran, M. Xue, Q. Fang, Y. Yan, V. Valtchev, S. Qiu, Fast, ambient temperature and pressure ionothermal synthesis of three-dimensional covalent organic frameworks, J. Am. Chem. Soc. 140 (2018) 4494–4498.

[141] M.B. Gawande, S.N. Shelke, R. Zboril, R.S. Varma, Microwave-assisted chemistry: synthetic applications for rapid assembly of nanomaterials and organics, Acc. Chem. Res. 47 (2014) 1338–1348.

[142] M. Nüchter, B. Ondruschka, W. Bonrath, A. Gum, Microwave assisted synthesis–a critical technology overview, Green Chem 6 (2004) 128–141.

[143] L.K. Ritchie, A. Trewin, A. Reguera-Galan, T. Hasell, A.I. Cooper, Synthesis of COF-5 using microwave irradiation and conventional solvothermal routes, Microporous Mesoporous Mater 132 (2010) 132–136.

[144] N.L. Campbell, R. Clowes, L.K. Ritchie, A.I. Cooper, Rapid microwave synthesis and purification of porous covalent organic frameworks, Chem. Mater. 21 (2009) 204–206.

[145] J.H. Bang, K.S. Suslick, Applications of ultrasound to the synthesis of nanostructured materials, Adv. Mater. 22 (2010) 1039–1059.

[146] S.T. Yang, J. Kim, H.Y. Cho, S. Kim, W.S. Ahn, Facile synthesis of covalent organic frameworks COF-1 and COF-5 by sonochemical method, RSC Adv 2 (2012) 10179–10181.

[147] J. Yoo, S. Lee, S. Hirata, C. Kim, C.K. Lee, T. Shiraki, N. Nakashima, J.K. Shim, In situ synthesis of covalent organic frameworks (COFs) on carbon nanotubes and graphenes by sonochemical reaction for CO_2 adsorbents, Chem. Lett. 44 (2015) 560–562.

[148] T. Friić, New opportunities for materials synthesis using mechanochemistry, J. Mater. Chem. 20 (2010) 7599–7605.

[149] S.L. James, C.J. Adams, C. Bolm, D. Braga, P. Collier, T. Frisč˘, F. Frisč˘ic´, F. Grepioni, K.D.M. Harris, G. Hyett, W. Jones, A. Krebs, J. Mack, L. Maini, A.G. Orpen, I.P. Parkin, W.C. Shearouse, J.W. Steed, D.C. Waddell, Mechanochemistry: opportunities for new and cleaner synthesis, Chem. Soc. Rev. 41 (2012) 413–417.

[150] B.P. Biswal, S. Chandra, S. Kandambeth, B. Lukose, T. Heine, R. Banerjee, Mechanochemical synthesis of chemically stable isoreticular covalent organic frameworks, J. Am. Chem. Soc. 135 (2013) 5328–5331.

[151] X. Wang, R. Ma, L. Hao, Q. Wu, C. Wang, Z. Wang, Mechanochemical synthesis of covalent organic framework for the efficient extraction of benzoylurea insecticides, J. Chromatogr. A 1551 (2018) 1–9.

[152] S. Kim, H.C. Choi, Light-promoted synthesis of highly-conjugated crystalline covalent organic framework, Commun. Chem. 2 (2019) 60.

[153] S. He, T. Zeng, S. Wang, H. Niu, Y. Cai, Facile synthesis of magnetic covalent organic framework with three-dimensional bouquet-like structure for enhanced extraction of organic targets, ACS Appl. Mater. Interfaces 9 (2017) 2959–2965.

[154] Y. Liao, J. Li, A. Thomas, General route to high surface area covalent organic frameworks and their metal oxide composites as magnetically recoverable adsorbents and for energy storage, ACS Macro Lett 6 (2017) 1444–1450.

[155] C.X. Yang, C. Liu, Y.M. Cao, X.P. Yan, Facile room-temperature solution-phase synthesis of a spherical covalent organic framework for high-resolution chromatographic separation, Chem. Commun. 51 (2015) 12254–12257.

[156] J. Ozdemir, I. Mosleh, M. Abolhassani, L.F. Greenlee, R.R. Beitle, M.H. Beyzavi, Covalent organic frameworks for the capture, fixation, or reduction of CO_2, Front. Energy Res. 7 (2019) 77.

[157] H. Furukawa, O.M. Yaghi, Storage of hydrogen, methane, and carbon dioxide in highly porous covalent organic frameworks for clean energy applications, J. Am. Chem. Soc. 131 (2009) 8875–8883.

[158] Z. Kahveci, T. Islamoglu, G.A. Shar, R. Ding, H.M. El-Kaderi, Targeted synthesis of a mesoporous triptycene-derived covalent organic framework, CrystEngComm 15 (2013) 1524–1527.

[159] Y. Zhao, K.X. Yao, B. Teng, T. Zhang, Y. Han, A perfluorinated covalent triazine-based framework for highly selective and water-tolerant CO_2 capture, Energy Environ. Sci. 6 (2013) 3684–3692.

[160] W. Yu, S. Gu, Y. Fu, S. Xiong, C. Pan, Y. Liu, G. Yu, Carbazole-decorated covalent triazine frameworks: novel nonmetal catalysts for carbon dioxide fixation and oxygen reduction reaction, J. Catal. 362 (2018) 1–9.

[161] O. Buyukcakir, S.H. Je, S.N. Talapaneni, D. Kim, A. Coskun, Charged covalent triazine frameworks for CO_2 capture and conversion, ACS Appl. Mater. Interfaces 9 (2017) 7209–7216.

[162] V. Saptal, D.B. Shinde, R. Banerjee, B.M. Bhanage, State-of-the-art catechol porphyrin COF catalyst for chemical fixation of carbon dioxide: via cyclic carbonates and oxazolidinones, Catal. Sci. Technol. 6 (2016) 6152–6158.

[163] N. Huang, X. Chen, R. Krishna, D. Jiang, wo-dimensional covalent organic frameworks for carbon dioxide capture through channel-wall functionalization, Angew. Chem. Int. Ed. 54 (2015) 2986–2990.

[164] N. Huang, R. Krishna, D. Jiang, Tailor-made pore surface engineering in covalent organic frameworks: systematic functionalization for performance screening, J. Am. Chem. Soc. 137 (2015) 7079–7082.

[165] Y. Te Liao, S. Dutta, C.H. Chien, C.C. Hu, F.K. Shieh, C.H. Lin, K.C.W. Wu, Synthesis of mixed-ligand zeolitic imidazolate framework (ZIF-8-90) for CO_2 adsorption, J. Inorg. Organomet. Polym. Mater. 25 (2015) 251–258.

[166] E. Haque, M.M. Islam, E. Pourazadi, S. Sarkar, A.T. Harris, A.I. Minett, E. Yanmaz, S.M. Alshehri, Y. Ide, K.C.W. Wu, Y.V. Kaneti, Y. Yamauchi, D M.S.A. Hossain, Boron-functionalized graphene oxide-organic frameworks for highly efficient CO_2 capture, Chem. Asian J. 12 (2017) 283–288.

[167] J.Y. Wu, M.G. Mohamed, S.W. Kuo, Directly synthesized nitrogen-doped microporous carbons from polybenzoxazine resins for carbon dioxide capture, Polym. Chem. 8 (2017) 5481–5489.

[168] M.G. Mohamed, X. Zhang, T.H. Mansoure, A.F.M. EL-Mahdy, C.F. Huang, M. Danko, Z. Xin, S.W. Kuo, Hypercrosslinked porous organic polymers based on tetraphenylanthraquinone for CO_2 uptake and high-performance supercapacitor, Polymer (Guildf) 205 (2020) 122857.

[169] M.M. Samy, M.G. Mohamed, S.W. Kuo, Directly synthesized nitrogen-and-oxygen–doped microporous carbons derived from a bio-derived polybenzoxazine exhibiting high-performance supercapacitance and CO_2 uptake, Eur. Polym. J. 138 (2020) 109954.

[170] Y. Zhang, S.N. Riduan, Functional porous organic polymers for heterogeneous catalysis, Chem. Soc. Rev. 41 (2012) 2083–2094.

[171] S.F. Anis, A. Khalil, G.Singaravel Saepurahman, R. Hashaikeh, A review on the fabrication of zeolite and mesoporous inorganic nanofibers formation for catalytic applications, Microporous Mesoporous Mater. 236 (2016) 176–192.

[172] L. Ma, C. Abney, W. Lin, Enantioselective catalysis with homochiral metal–organic frameworks, Chem. Soc. Rev. 38 (2009) 1248–1256.

[173] Y. Wen, J. Zhang, Q. Xu, X.T. Wu, Q.L. Zhu, Pore surface engineering of metal–organic frameworks for heterogeneous catalysis, Coord. Chem. Rev. 376 (2018) 248–276.

[174] M. Wang, H. Guo, R. Xue, Q. Li, H. Liu, N. Wu, W. Yao, W. Yang, Covalent organic frameworks: a new class of porous organic frameworks for supercapacitor electrodes, ChemElectroChem 6 (2019) 2984–2987.

[175] S. Cao, B. Li, R. Zhu, H. Pang, Design and synthesis of covalent organic frameworks towards energy and environment fields, Chem. Eng. J. 355 (2019) 602–623.

[176] C.R. Deblase, K. Hernández-Burgos, K.E. Silberstein, G.G. Rodríguez-Calero, R.P. Bisbey, H.D. Abruña, W.R. Dichtel, Rapid and efficient redox processes within 2D covalent organic framework thin films, ACS Nano 9 (2015) 3178–3183.

[177] M.G. Mohamed, A.F.M. EL-Mahdy, M.M.M. Ahmed, S.W. Kuo, Direct synthesis of microporous bicarbazole-based covalent triazine frameworks for high-performance energy storage and carbon dioxide uptake, Chempluschem 84 (2019) 1767–1774.

[178] A.F.M. El-Mahdy, M.G. Mohamed, T.H. Mansoure, H.H. Yu, T. Chen, S.W. Kuo, Ultrastable tetraphenyl-p-phenylenediamine-based covalent organic frameworks as platforms for high-performance electrochemical supercapacitors, Chem. Commun. 55 (2019) 14890–14893.

[179] M. Dogru, T. Bein, On the road towards electroactive covalent organic frameworks, Chem. Commun. 50 (2014) 5531–5546.

[180] S. Wan, J. Guo, J. Kim, H. Ihee, D. Jiang, A belt-shaped, blue luminescent, and semiconducting covalent organic framework, Angew. Chem. Int. Ed. 47 (2008) 8826–8830.

[181] X. Feng, L. Liu, Y. Honsho, A. Saeki, S. Seki, S. Irle, Y. Dong, A. Nagai, D. Jiang, High-Rate Charge-Carrier Transport in Porphyrin Covalent Organic Frameworks: switching from Hole to Electron to Ambipolar Conduction, Angew. Chem. Int. Ed. 51 (2012) 2618–2622.

[182] X. Chen, M. Addicoat, E. Jin, L. Zhai, H. Xu, N. Huang, Z. Guo, L. Liu, S. Irle, D. Jiang, Locking covalent organic frameworks with hydrogen bonds: general and remarkable effects on crystalline structure, physical properties, and photochemical activity, J. Am. Chem. Soc. 137 (2015) 3241–3247.

[183] X. Ding, J.J. Guo, X. Feng, Y. Honsho, J.J. Guo, S. Seki, P. Maitarad, A. Saeki, S. Nagase, D. Jiang, Synthesis of metallophthalocyanine covalent organic frameworks that exhibit high carrier mobility and photoconductivity, Angew. Chem. Int. Ed. 50 (2011) 1289–1293.

[184] X. Ding, X. Feng, A. Saeki, S. Seki, A. Nagai, D. Jiang, Conducting metallophthalocyanine 2D covalent organic frameworks: the role of central metals in controlling π-electronic functions, Chem. Commun. 48 (2012) 8952–8954.

[185] X. Feng, L. Chen, Y. Honsho, O. Saengsawang, L. Liu, L. Wang, A. Saeki, S. Irle, S. Seki, Y. Dong, D. Jiang, An ambipolar conducting covalent organic framework with self-sorted and periodic electron donor-acceptor ordering, Adv. Mater. 24 (2012) 3026–3031.

[186] M. Dogru, M. Handloser, F. Auras, T. Kunz, D. Medina, A. Hartschuh, P. Knochel, T. Bein, A photoconductive thienothiophene-based covalent organic framework showing charge transfer towards included fullerene, Angew. Chem. Int. Ed. 52 (2013) 2920–2924.

[187] D. Cui, D.F. Perepichka, J.M. MacLeod, F. Rosei, Surface-confined single-layer covalent organic frameworks: design, synthesis and application, Chem. Soc. Rev. 49 (2020) 2020–2038.

[188] H. Ding, Y. Li, H. Hu, Y. Sun, J. Wang, C. Wang, C. Wang, G. Zhang, B. Wang, W. Xu, D. Zhang, A tetrathiafulvalene-based electroactive covalent organic framework, Chem. Eur. J. 20 (2014) 14614–14618.

[189] S.L. Cai, Y.B. Zhang, A.B. Pun, B. He, J. Yang, F.M. Toma, I.D. Sharp, O.M. Yaghi, J. Fan, S.R. Zheng, W.G. Zhang, Y. Liu, Tunable electrical conductivity in oriented thin films of tetrathiafulvalene-based covalent organic framework, Chem. Sci. 5 (2014) 4693–4700.

[190] C. Poelking, M. Tietze, C. Elschner, S. Olthof, D. Hertel, B. Baumeier, F. Würthner, K. Meerholz, K. Leo, D. Andrienko, Impact of mesoscale order on open-circuit voltage in organic solar cells, Nat. Mater. 14 (2015) 434–439.

[191] D.D. Medina, M.L. Petrus, A.N. Jumabekov, J.T. Margraf, S. Weinberger, J.M. Rotter, T. Clark, T. Bein, Directional charge-carrier transport in oriented benzodithiophene covalent organic framework thin films, ACS Nano 11 (2017) 2706–2713.

[192] M.G. Mohamed, C.C. Lee, A.F.M. EL-Mahdy, J. Lüder, M.H. Yu, Z. Li, Z. Zhu, C.C. Chueh, S.W. Kuo, Exploitation of two-dimensional conjugated covalent organic frameworks based on tetraphenylethylene with bicarbazole and pyrene units and applications in perovskite solar cells, J. Mater. Chem. A 8 (2020) 11448–11459.

[193] J.M. Cox, B. Mileson, A. Sadagopan, S.A. Lopez, Molecular recognition and band alignment in 3D covalent organic frameworks for cocrystalline organic photovoltaics, J. Phys. Chem. C 124 (2020) 9126–9133.

[194] S. Park, M.S. Kim, W. Jang, J.K. Park, D.H. Wang, Covalent organic nanosheets for effective charge transport layers in planar-type perovskite solar cells, Nanoscale 10 (2018) 4708–4717.

[195] B. Xu, S. Li, H. Jiao, J. Yin, Z. Liu, W. Zhong, A two-dimensional quinazoline based covalent organic framework with a suitable direct gap and superior optical absorption for photovoltaic applications, J. Mater. Chem. A 8 (2020) 3865–3871.

[196] Y. Liu, M.O. Keeffe, M.M.J. Treacy, O.M. Yaghi, The geometry of periodic knots, polycatenanes and weaving from a chemical perspective: a library for reticular chemistry, Chem. Soc. Rev. 47 (2018) 4642–4664.

[197] M.G. Mohamed, E.C. Ataydo, B.M. Matsagar, J. Na, Y. Yamauchi, K.C.W. Wu, S.W. Kuo, Construction hierarchically mesoporous/microporous materials based on block copolymer and covalent organic framework, J. Taiwan Inst. Chem. Eng. 112 (2020) 180–192.

[198] J. Luo, X. Sun, J. Yin, P. Yin, T. Liu, Supramolecular nanostructures constructed from cluster-based hybrid macromolecules, Giant 2 (2020) 100013.

[199] Y. Liu, T. Liu, X. Yan, Q. Guo, J. Wang, R. Zhang, S. Zhang, Z. Su, J. Huang, G. Liu, W. Zhang, W. Zhang, T. Aida, K. Yue, M. Huang, S.Z.D. Cheng, Mesoatom alloys via self-sorting approach of giant molecules blends, Giant 4 (2020) 100031.

[200] Z. Su, R. Zhang, X. Yan, Q. Guo, J. Huang, W. Shan, Y. Liu, M. Huang, S.Z.D. Cheng, The role of architectural engineering in macromolecular self-assemblies via non-covalent interactions: a molecular LEGO approach, Prog. Polym. Sci. 103 (2020) 101230.